

SPECIAL FEATURE: TUTORIAL

Ion activation methods for tandem mass spectrometry

Lekha Sleno and Dietrich A. Volmer*

National Research Council, Institute for Marine Biosciences, 1411 Oxford Street, Halifax, Nova Scotia, Canada, B3H 3Z1

Received 20 December 2003; Accepted 8 August 2004

This tutorial presents the most common ion activation techniques employed in tandem mass spectrometry. In-source fragmentation and metastable ion decompositions, as well as the general theory of unimolecular dissociations of ions, are initially discussed. This is followed by tandem mass spectrometry, which implies that the activation of ions is distinct from the ionization step, and that the precursor and product ions are both characterized independently by their mass/charge ratios. In collision-induced dissociation (CID), activation of the selected ions occurs by collision(s) with neutral gas molecules in a collision cell. This experiment can be done at high (keV) collision energies, using tandem sector and time-of-flight instruments, or at low (eV range) energies, in tandem quadrupole and ion trapping instruments. It can be performed using either single or multiple collisions with a selected gas and each of these factors influences the distribution of internal energy that the activated ion will possess. While CID remains the most common ion activation technique employed in analytical laboratories today, several new methods have become increasingly useful for specific applications. More recent techniques are examined and their differences, advantages and disadvantages are described in comparison with CID. Collisional activation upon impact of precursor ions on solid surfaces, surface-induced dissociation (SID), is gaining importance as an alternative to gas targets and has been implemented in several different types of mass spectrometers. Furthermore, unique fragmentation mechanisms of multiply-charged species can be studied by electron-capture dissociation (ECD). The ECD technique has been recognized as an efficient means to study non-covalent interactions and to gain sequence information in proteomics applications. Trapping instruments, such as quadrupole ion traps and Fourier transform ion cyclotron resonance instruments, are particularly useful for the photoactivation of ions, specifically for fragmentation of precursor ions by infrared multiphoton dissociation (IRMPD). IRMPD is a non-selective activation method and usually yields rich fragmentation spectra. Lastly, blackbody infrared radiative dissociation is presented with a focus on determining activation energies and other important parameters for the characterization of fragmentation pathways. The individual methods are presented so as to facilitate the understanding of each mechanism of activation and their particular advantages and representative applications. Copyright © 2004 John Wiley & Sons, Ltd.

KEYWORDS: tandem mass spectrometry; ion activation; collision-induced dissociation; surface-induced dissociation; electron capture dissociation; infrared multiphoton dissociation; blackbody infrared radiative dissociation

INTRODUCTION

The field of mass spectrometry, over the past half century, has evolved into an essential technique with numerous chemical and biological applications. In simple terms, it comprises the study of ionized molecules and their reactions in the gas phase within a mass spectrometer. Early mass spectrometers were capable of only one stage of mass analysis and structure elucidation relied on dissociation of the molecular

ion in the course of its formation and within the confines of the ion source. These instruments were very useful, but only for a limited range of molecules, viz. low molecular mass, volatile compounds. Soft ionization techniques, such as fast atom bombardment (FAB),¹ electrospray ionization (ESI),^{2,3} and matrix-assisted laser desorption/ionization (MALDI),⁴ subsequently extended the range of application of mass spectrometry to polar, thermally labile compounds. Unfortunately, these ionization techniques primarily yield protonated or deprotonated species with little or no fragmentation occurring in the source, therefore limiting the structural information available in a single-stage mass spectrum. As a consequence, tandem mass spectrometry has

*Correspondence to: Dietrich A. Volmer, National Research Council, Institute for Marine Biosciences, 1411 Oxford Street, Halifax, Nova Scotia, Canada, B3H 3Z1.
E-mail: dietrich.volmer@nrc-cnrc.gc.ca

emerged as an essential technique for the structural analysis of a wide range of biologically relevant compounds, such as pharmaceutical drugs, peptides and proteins, and nucleic acids. Tandem mass spectrometry involves the activation of a known precursor ion formed in the ion source and the mass analysis of its fragmentation products. The ion activation step is crucial to the experiment and ultimately defines what types of products result. Several ion activation techniques have been developed. Early experiments mainly studied metastable ion decompositions. Next, collision-induced dissociation (CID) was introduced and is still employed in most tandem mass spectrometry applications today. Several relatively new techniques have been designed to complement conventional CID spectra. A detailed description of each of these activation methods is presented in this tutorial.

Starting with a brief introduction to unimolecular dissociations occurring in the high-vacuum conditions of a mass spectrometer, a fundamental discussion on metastable decompositions is provided together with a description of how they are utilized in sector and time-of-flight (TOF) instruments. This is followed by a description of CID in several other types of mass spectrometers. Electron capture dissociation (ECD), along with its specific uses and advantages, is then introduced. Finally, infrared excitation techniques such as infrared multiphoton dissociation (IRMPD) and blackbody infrared radiative dissociation (BIRD) are discussed. Several of these activation techniques can provide complementary information on ion fragmentation in a mass spectrometer and looking at the individual activation mechanisms helps the reader understand what each method can offer. Table 1 briefly describes the ion activation methods, their relevant collision energies and the instruments in which these experiments are most commonly performed.

UNIMOLECULAR DISSOCIATION

Before we discuss the specifics of each ion activation technique, we must first introduce the basic theories used

to describe the behavior of an ionized molecule under the conditions of a mass spectrometer, after it has been activated. In conventional EI instruments, all processes occur in high vacuum (at pressures that are typically 10^{-5} Torr and may be as low as 10^{-9} Torr (1 Torr = 133.3 Pa)), virtually eliminating the possibility of collisions between ions and neutral molecules. First, an electron beam ionizes the molecule generating a radical ion. An accelerating voltage (V_{acc}) is applied and the electric field directs the resulting ions towards the mass analyzer. All ions receive the same amount of kinetic energy (E_k) per charge such that the ion kinetic energy $E_k = \frac{1}{2}mv^2 = zV_{acc}$, where m is the mass of the ionized molecule, v is the velocity of the ion and z is its charge. A 70 eV electron beam is usually used in the initial ionization step. Interaction between the molecule and the electron beam most often imparts excess energy above the ionization threshold of the molecule. The distribution of internal energies of the population of molecular ions, $P(E)$, is a key parameter; however it is rarely definable. In the collision-free environment there is no exchange of energy between the activated ions and hence no thermal equilibrium. Moreover, the very short ionization step promoting the molecule to an excited electronic state is followed by internal energy redistribution into different vibrational modes. The resulting ion, even if excited above the dissociation limit, may or may not undergo fragmentation. Within a short time-scale compared with the time spent in the source (10^{-6} s), the ion equilibrates its internal energy over all available quantum states, thus favoring internal conversion into ground electronic, vibrationally excited state species. Energy relaxation does not occur on the time-scale of most mass spectrometers; instead radiationless transitions occur, and the total energy of each (isolated) molecular ion stays constant.⁵ The resulting EI spectra are highly reproducible from one instrument to another, and therefore can be used to build databases of mass spectra for molecular identification.

Table 1. General description of different ion activation processes presented

Method	Energy Range	Instruments	Description
PSD	Low	RETOF	Metastable or collision-induced dissociations in flight tube of reflectron time-of-flight instrument
CID	Low	QqQ, IT, QqTOF, QqLIT, FTICR	Collision-induced dissociation by collision of precursor ions with inert target gas molecules in collision cell. Energy range 1–100 eV
	High	Tandem TOF, sectors	Same as above with keV energies
SID	Low	Hybrid (BqQ), QqQ, IT, FTICR	Collisions between precursor ions and solid target surface with or without self-assembled monolayer causing fragmentations as well as other side reactions
	High	Tandem TOF, RETOF	Same as above with precursors of higher translational energies (instrument dependent)
ECD	Low	FTICR	Low-energy beam of electrons resulting in electron capture at protonation (or cationic) site with subsequent fragmentation following radical ion chemistry
IRMPD	Low	IT, FTICR	Continuous-wave low-energy infrared laser activates precursor ions by multiphoton absorption with consequent fragmentation
BIRD	Low	IT, FTICR	Low-energy thermal activation method ideal for calculations of energy thresholds and thermodynamic properties

Observed fragmentations in EI result exclusively from unimolecular dissociations, a consequence of the high-vacuum conditions in the source. These types of fragmentations depend only on the structure and the total internal energy of the ionized molecule. The quasi-equilibrium theory (QET)⁶ or, equivalently, the Rice, Ramsperger Kassel and Marcus (RRKM)⁷ theory can be used to explain unimolecular dissociations in the gas phase under high vacuum. Assumptions of these theories state that all oscillator motion within an ion is independent, including electronic, translation, vibration and rotation, and that classical mechanics, with some corrections based on quantum mechanics, can explain nuclei movements. An important postulate maintains that all microscopic states have equal statistical probability and all the degrees of freedom participate with the same probability in the energy distribution. The whole system is described using a three-dimensional potential energy surface separating reactants and products with barriers which, when crossed, yield irreversible transformations. A representative potential energy surface is illustrated in Fig. 1.

Interaction of electrons with molecules and subsequent ionization in an EI source is very fast, taking $<10^{-16}$ s. This process forms molecular ions in ground and excited states. Ionization occurs by a vertical transition and is much faster than a vibration ($\sim 10^{-14}$ – 10^{-12} s), therefore the interatomic distances remain largely unchanged (Franck–Condon principle). Excited molecular ions redistribute their energy over the degrees of freedom in a statistical manner, determined by the intersections between the potential energy surfaces. The rate of redistribution depends on the number of these conical intersections and, for this reason, on the number of atoms in the ionized molecule. The transitions lead to lower electronic states (but the same total internal energy), resulting in the electronic ground state with a given total vibrational

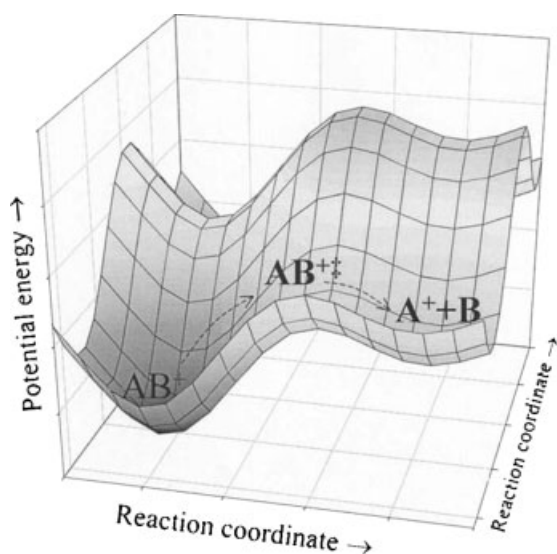


Figure 1. 3D potential energy surface illustrating possible dissociation pathways. Example: representative dissociation pathway is seen with precursor ion represented as AB^+ forming product ion A^+ and neutral B through a saddlepoint in the potential energy surface, designating the transition state for this dissociation pathway.

and rotational energy but a wide range when a population of molecular ions is considered. After the accumulation of internal energy into appropriate modes, fragmentation of the ion occurs. Molecular ions leaving the source can reach the detector intact or undergo metastable decompositions (see below).

Fragmentation reactions are defined by a characteristic threshold energy, E_0 . The RRKM theory provides an expression describing the internal energy-dependent rate constant for a fragmentation reaction:^{8,9}

$$k(E) = \frac{s}{h} \left[\frac{P^\ddagger(E - E_0)}{\rho_E} \right]$$

where h is Planck's constant, s is the number of equivalent routes for the reaction, E is the internal energy contained in the ion, with E_0 threshold energy for the transition, $P^\ddagger(E - E_0)$ represents the total number of states of activated complexes between zero and $(E - E_0)$ energy and ρ_E is the density of states of the ions at energy E . RRKM assumes that the dissociation rate constant depends for a particular molecule only on the internal energy present in the molecules. A molecule can only dissociate if it contains an internal energy above E_0 and the decomposition rate will obviously be faster the more excess energy is present within the molecule. A simplified expression based on QET or the equivalent RRKM theory can also be employed; however, it should be used with caution since inherent errors exist, particularly at low energy:

$$k(E) = \nu \left(\frac{E - E_0}{E} \right)^{n-1}$$

where n represents the number of vibrational degrees of freedom and ν is the frequency factor. The quantities of n , ν and E_0 depend on the structure of a molecule while ν is inversely related to the steric requirements of the reaction, viz. on whether the oscillators are free to vibrate/rotate in the activated complex or whether there are constraints (a 'tight' activated complex). The entropy factor for the transition state, ΔS^\ddagger , is obviously decreased when the activated complex is more ordered, thereby decreasing the frequency factor, as noted in the following expression, and hence decreasing the rate constant:

$$\nu = \left(\frac{E - E_0}{h} \right) e^{\Delta S^\ddagger/R}$$

A fragmentation reaction resulting from a transition state with defined conformation (tight complex) reduces ΔS^\ddagger , but can still occur since the threshold energy, E_0 , can be decreased by a favorable geometry of the transition state. For example, several fragmentation reactions occur via stable six-membered cyclic intermediates. One of these reactions for radical ions is known as the McLafferty rearrangement, but similar fragmentations occur with even-electron species.¹⁰ Figure 2 illustrates the difference between rearrangements and simple bond cleavages in terms of $k(E)$ curves as arbitrary internal energy functions. Tighter transition states are favorable at lower energies and the importance of

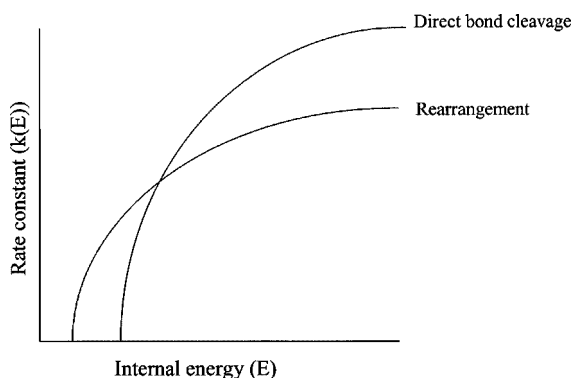


Figure 2. Arbitrary internal energy curves for rearrangement and simple bond cleavage fragmentation reactions.

fragmentations involving loose complexes increases with internal energy.¹¹

The rate constant for dissociation defines the behavior seen in the resulting mass spectra. Since an ion spends $\sim 10^{-6}$ s in the ion source, the ion is increasingly likely to fragment in the source if $k(E) > 10^6 \text{ s}^{-1}$. Furthermore, as the total time spent in mass spectrometers of many types is $\sim 10^{-5}$ s (although it is longer in trapping instruments), a fragmentation reaction with a rate constant $k(E) < 10^5 \text{ s}^{-1}$ can be expected to be detected as the molecular ion.¹⁰ In the case where the rate constant $k(E)$ equals the reciprocal of the ion residence time, $\sim 10^{-5}$ s, these ions have a good chance of dissociating *en route* between the ion source and the detector. These ions are known as metastable ions and the resulting signals collected in magnetic mass spectrometers are known as metastable peaks. This special circumstance applies to only a small proportion of ions in the population originally produced. Many mass spectrometrists have taken advantage of metastable peaks for studying the fragmentation behavior of their molecules more closely. Figure 3 illustrates the relative portions of stable, metastable and unstable ions in an internal energy distribution curve.

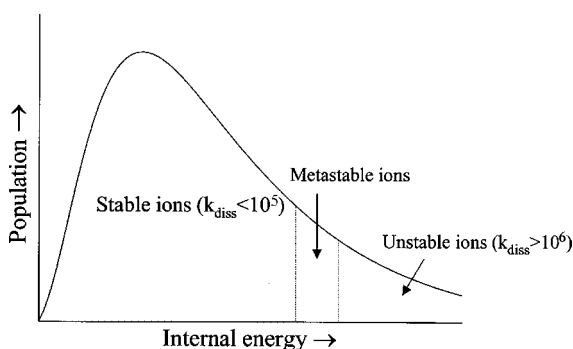


Figure 3. Hypothetical distribution of internal energies of ions formed in a typical beam-type instrument. Ions with dissociation rate constants $< 10^5 \text{ s}^{-1}$ remain intact on the time-scale of the mass spectrometer (10^{-5} s). Those with rate constants $> 10^6 \text{ s}^{-1}$ are unstable ions and fragment in the ion source, while the intermediate situation ($10^6 \text{ s}^{-1} > k_{\text{diss}} > 10^5 \text{ s}^{-1}$) represents metastable ions that fragment between the source and the detector.

METASTABLE ION DECOMPOSITIONS

Molecular ions formed in the ion source having sufficient internal energy to fragment spontaneously in a field-free region between the source and the analyzer are classified as metastable ions. These fragments were initially identified as unknown broadened peaks in the earliest mass spectra¹² and later explained as unimolecular decay products formed in the field-free regions of a mass spectrometer.¹³ All ions leaving the ion source have approximately equal kinetic energy and their masses can be differentiated based on their flight velocities. In the original double focusing mass spectrometers, the electrostatic analyzer (E) is placed in front of the magnetic analyzer (B) in what is known as the Nier–Johnson geometry. Metastable product ions formed between the ion source and the E sector are not seen in the mass spectrum, since the electric sector distinguishes ions based on kinetic energy to charge ratio and therefore does not transmit these products. Such an instrument does exhibit metastable peaks for fragments formed in the field-free region between the two sectors. Metastable peaks, however, are not observed at m/z values representing the true fragment ion mass, but instead appear at non-integer m/z values between the actual product ion and its precursor. This is due to their lower than normal kinetic energies and the fact that a magnetic sector actually analyzes momentum not mass unless all ions have the same kinetic energy. This can be explained through a simple derivation. Recall that the energy of the precursor ion is equal to $\frac{1}{2}mv^2 = zV_{\text{acc}}$. As an ion of mass m_p leaves the electrostatic sector, it has a velocity v_p , such that

$$v_p = \sqrt{\frac{2zV_{\text{acc}}}{m_p}}$$

The law of momentum conservation states that the precursor ion's momentum, $m_p v_p$, must be shared between the products of decomposition. If a precursor, m_p^+ , dissociates into a fragment ion, m_f^+ , the resulting neutral would have mass $(m_p - m_f)$, considering all species as singly charged:

$$m_p v_p = m_f v_f + (m_p - m_f) v_f$$

Assuming identical velocities for the precursor and its products ($v_f = v_p = v$), the momentum has consequently been altered:

$$m_f v = m_f \sqrt{\frac{2zV_{\text{acc}}}{m_p}}$$

Let us now consider what happens to the motion of m_f^+ in the magnetic field of the sector instrument. There are two forces acting on the ion in the sector. The centrifugal force on the ion must balance the force preventing its ejection off on a tangent, which is achieved by applying the magnetic field:

$$\frac{m_f v^2}{r_b} = Bzv$$

where r_b is the radius of the ion's trajectory in the magnetic analyzer. As a result, if we combine the two above equations, we end up with the following relation:

$$\frac{m_f^2}{m_p z} = \frac{B^2 r_b^2}{2V_{\text{acc}}}$$

Since the mass analysis equation for magnetic sector instruments is

$$\frac{m}{z} = \frac{B^2 r^2}{2V_{\text{acc}}}$$

the apparent mass of the metastable product ion, m^* , is given by

$$m^* = \frac{m_f^2}{m_p}$$

This equation clarifies why metastable peaks always appear at m/z values lower than m_f .

This relationship has the advantage that one can easily assemble fragmentation pathways using these metastable peaks, which is illustrated in Fig. 4 with the metastable spectrum of theobromine (a purine derivative) obtained using an EB sector instrument.^{14,15} Metastable peaks are usually distinguishable from other peaks within the mass spectrum since the kinetic energy released during the fragmentation leads to a dispersion of velocities which reduces the resolution observed. When a precursor dissociates during the flight, fragment ions are ejected in all directions, resulting in the products being formed with a distribution of velocity components.

Before we describe techniques for the detection of metastable ions in sector instruments, let us look at the situation in the TOF mass spectrometer, which is much simpler to understand. In a TOF instrument, if an ion fragments within the source, the precursor and product ions acquire the same kinetic energy and thus can be differentiated by their velocities and flight times, which are related to

their respective masses (strictly, mass/charge ratios). When a precursor ion enters the flight tube of a TOF analyzer, post-source decay (PSD) of ions (viz. metastable ion dissociation) yields decomposition products reaching a linear detector with the same velocity as the original precursor ion. Hence, in TOF-MS, ions that decompose during their flight through the drift tube are usually detected at the precursor's m/z . These products can be distinguished, however, by the application of a reflectron-TOF (RETOF).^{16,17} All ions enter the retarding field of the reflectron but the lighter ones penetrate less than the heavier ones. Fragment ions therefore exit the reflectron earlier than their precursors and therefore have characteristic flight times based on their masses. The PSD technique is used extensively with matrix-assisted laser desorption/ionization (MALDI)-RETOF instruments.¹⁶ MALDI is considered to be a soft ionization method given that in-source fragmentation is usually minimal under standard conditions.^{4,18} Since the entire flight tube is a field-free region, metastable decompositions have up to several microseconds to occur and thus fragment ions are often more abundant in these than in sector instruments. At present, however, PSD experiments frequently make use of a collision cell placed between the ionization source and the drift tube to induce fragmentation by collision with a neutral target gas (see below). The mass of the precursor can be found when the instrument is operated in the linear mode, where the fragment ions are detected at the precursor ion's m/z value, and subsequent switching to the reflectron mode identifies the products formed. Most instruments include a precursor ion selection step for the ions undergoing PSD. A low-resolution precursor ion-selecting device cuts out a certain time slice of ions, corresponding

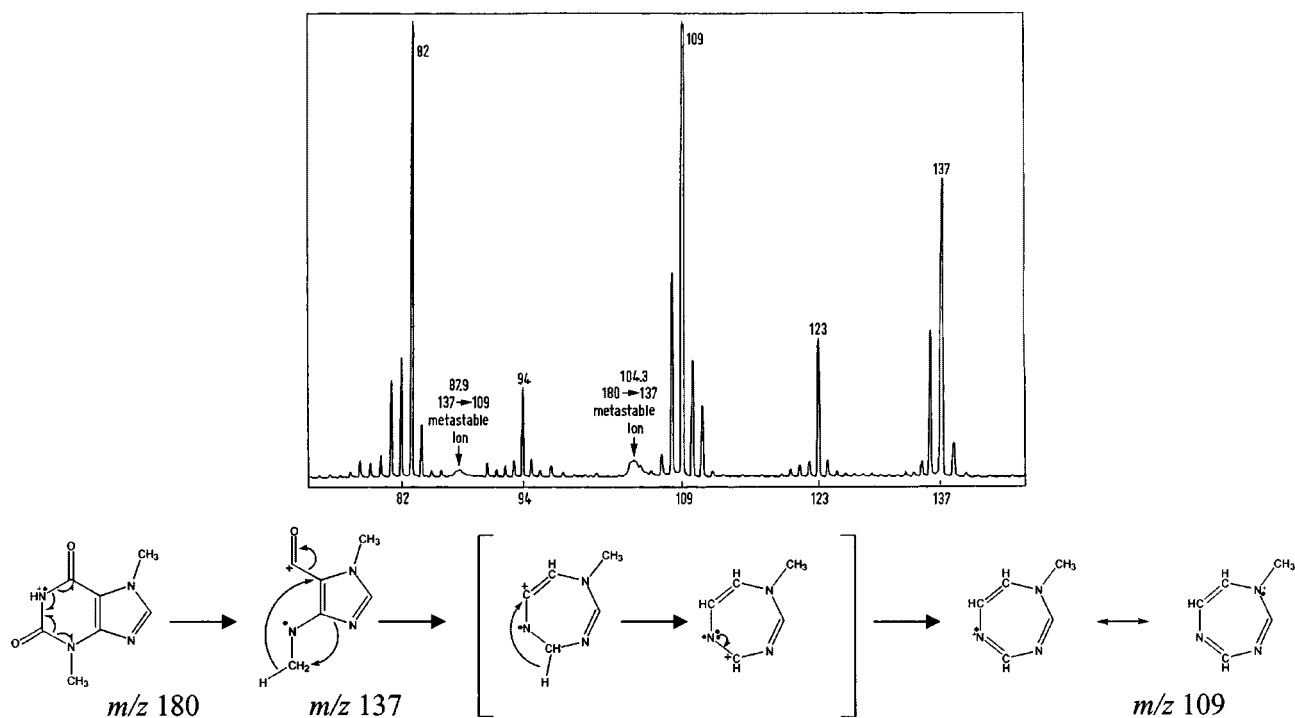


Figure 4. Metastable ion spectra of theobromine (a purine derivative) exhibiting useful fragment relationships for structural analysis. Metastable peaks are seen at m/z 104.3 and 87.9, corresponding to transitions m/z 180 → 137 and 137 → 109, respectively. Metastable analyses, as in this example, allow fragmentation pathways to be elucidated more easily. From Ref. 14 (reproduced by courtesy of John Wiley and Sons) (fragmentation scheme above proposed by present authors).

to a small range of m/z values.¹⁶ MALDI-PSD can be a very sensitive technique and signal-to-noise ratios are often improved over those recorded using more conventional instruments employed for the analysis of metastable ions.¹⁹

PSD applications have mainly involved peptide and protein analysis. This technique can be compared with CID for peptide fragmentation patterns. Indeed, there are several similarities between the spectra from both methods but also some interesting differences, including the lack of side-chain cleavages, in contrast to high-energy CID, and the predominance of product ions including additional ammonia losses in PSD spectra.¹⁷ Figure 5 shows the complete PSD fragment ion spectrum of substance P, as an example for the specific cleavages of peptide ions.¹⁷ The fragment ion nomenclature denotes cleavages of the C_α —CO and peptide bond for *a*- and *b*-type ions, respectively.

Let us now venture back to specific scan modes for detecting metastable ion decompositions in sector instruments. Keep in mind, though, that these scans can also be combined with a collision cell placed between the two sectors for CID. Beynon *et al.*,²⁰ in the early 1970s, used a reverse geometry sector instrument (BE geometry) for mass-analysed ion kinetic energy spectroscopy (MIKES), which is still employed today for specific applications.^{21,22} Recall that at the source outlet, every singly charged species has equal kinetic energy, which is constant throughout its flight. If dissociation occurs between the magnetic and electrostatic sectors, fragments retain the parent velocity, v_p . In the electrostatic analyser, all ions must obey the condition $zE = mv^2/r_e$, where r_e is the radius of the ion's trajectory in the electric field, z is the charge on the ion and E is the electric field applied. E remains constant for all precursor ions, since they all have the same kinetic energy. This condition is derived from the fact that the electric force (zE) must be balanced by the centrifugal force (mv^2/r_e). Metastables are normally eliminated from the spectrum, since the electrostatic sector separates ions based on their different kinetic energies, thus differentiating precursor and fragment ions. A modification of the electric field, E , can be made so that

$$zE_p = \frac{m_p v_p^2}{r_e} \text{ and } zE_f = \frac{m_f v_p^2}{r_e}$$

If E is scanned, a metastable peak is observed when $E = E_f$. Since $E_p/E_f = m_p/m_f$, the fragment masses are proportional to the electric fields at which they are detected and the electric field scale for the electrostatic sector corresponds to a mass scale. In brief, we can isolate a beam of precursor ions with a constant B value in the magnetic sector and scan E for the determination of metastable fragment ion masses. It should be noted that energy is converted from internal modes to kinetic energy during fragmentation giving the fragment ion a distribution of velocities about the average value of v_p . A MIKES experiment allows not only the study of fragmentation pathways, but also a direct measurement of this kinetic energy released during the fragmentation between the two sectors by measuring the width of the resulting peak.²³ This can also be done by scanning the accelerating voltage, V_{acc} .²³

Several scan types can be used for recording the products of metastable or CID. These have value for both fundamental studies of the structures of gas-phase ions and in analytical applications to the analysis of mixtures. The most common of these is the *product ion scan*. It involves the selection of a specific precursor ion for fragmentation. This can be achieved by using a double focusing mass spectrometer of reverse geometry in which a B sector precedes an E sector. The B-field is used to select the precursor ion and the E-field is used to scan the products generated between the two fields. Alternatively, a forward geometry instrument can be scanned so the ratio B/E is a constant to record the same information. The ratio of B/E required to pass the precursor ion and product ions is constant as both the B and E field values are decreased from their original values. All product ions of the selected precursor can be detected with the same B/E ratio.^{24,25} The B/E linked scan is useful in both EB and BE geometry instruments and the resolution is enhanced as compared to the MIKES experiment. In this case, only product ions formed with zero kinetic energy will be focused by both sectors and subsequently detected. An alternative scan, the B^2/E constant scan is useful for identifying a family of compounds present in a mixture.²⁶ Initial values of B and E are set in order to focus selected fragment ions formed in the source. In this experiment, the two sectors are scanned together while keeping B^2/E constant. Yet another technique, the *accelerating voltage scan* (defocusing method),^{23,25} can be

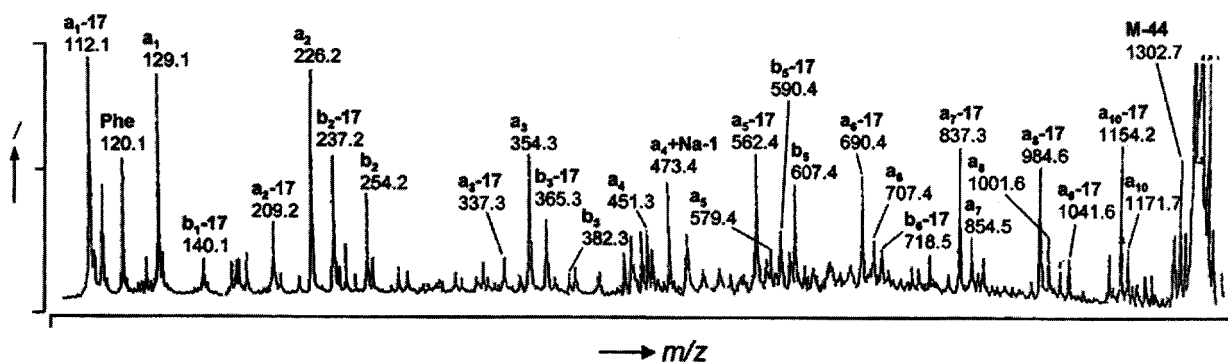


Figure 5. MALDI PSD fragment ion spectrum of substance P ($M = 1347.7$). The spectrum is composed of 14 separate segments, each resulting from 50 single laser shots. (Note that the x - and y -axes do not follow a simple function in a two-stage RETOF. Thus, the fragment ion signals are individually mass assigned). Predominant cleavages exhibit *a*- and *b*-type ions as well as corresponding ions with ammonia losses. Adapted from Ref. 17 by courtesy of Elsevier Science.

used to determine the precursor ions for a given fragment formed in the source of a single focusing instrument. In short, the instrument is first focused on a certain fragment ion with a source potential V_{acc} , which is then progressively increased. The selected fragment ion is 'defocused' if it is produced in the source, but is detected every time V_{acc} reaches a value corresponding to any precursor of the given fragment ion. Finally, the last scan that will be mentioned is the *constant neutral loss scan*.²⁷ This rather complicated scan is used for the selective detection of specific classes of compounds, which exhibit a common neutral mass, m_n , being lost during fragmentation. If both B and E sectors are scanned together, with the ratio $B_1^2(1 - E')/E^2$ remaining constant, fragments formed in a field-free region are focused by both sectors only if they coincide with some constant neutral loss specific to the experiment. Even though rather complex methods are used to detect specific types of products, it must be noted that there are only a limited number of basic scan types. In a two-stage (MS/MS) experiment these are the precursor scan, product scan, neutral loss scan and reaction monitoring experiment, which are summarized symbolically in Fig. 6.

The study of ion decompositions using the above scans has allowed the confirmation of fragmentation pathways. Important limitations remain with metastable decompositions, however, given that no control over fragmentation occurs. Also, these instruments and the necessary scans are complicated and, hence, are not very practical for analytical laboratories with routine requirements. Accordingly, most tandem mass spectrometry applications presently use CID in more modern instruments, such as triple quadrupoles and ion traps. The basic principles of this ion activation technique are explained in the next section.

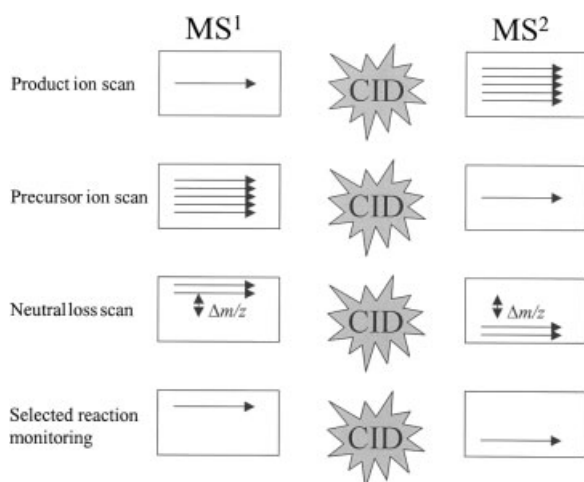


Figure 6. Basic scan modes used in CID experiments. For a product ion scan, the first mass analyzer selects a specific precursor ion while the second scans through a certain m/z range. A precursor ion scan involves scanning the first analyzer while detecting only one specific product ion. In a neutral loss experiment, both analyzers are scanned together so as to allow precursor and product ion pairs which have a defined m/z shift to be analyzed. A selected *reaction monitoring scan* specifies both the precursor and product ion for the detection of only one pair at the detector.

COLLISION-INDUCED DISSOCIATION

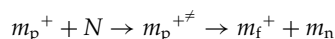
As shown in the previous section, the ability to characterize precursor ions from metastable dissociations alone is fairly limited. Methods that cause ion activation increase internal energy and thus increase the number of precursors that dissociate in addition to providing structurally informative fragments. CID remains the most common ion activation method used in present day instruments.^{28–30} Collisions between the precursor ion and a neutral target gas are accompanied by an increase in internal energy, which induces decomposition with much improved probability of fragmentation as compared with metastable unimolecular dissociations. A brief review of the collision process between a fast ion and slow target is useful for understanding how the collision energy is converted into internal energy. When an ion with a high translational energy undergoes an inelastic collision with a neutral, part of the translational energy is converted into internal energy of the ion, leading to subsequent decomposition.³¹ The transfer of kinetic energy to internal energy can be represented by the laws of physics involving a mobile species (ion) and a static target (gas). To simplify the description of such a process, it is more useful to work in the center-of-mass (com) framework instead of the laboratory reference frame. In the latter, a binary collision is described by the two separate particles involved with their individual position and velocity vectors. A conversion to the com reference frame makes the situation easier to describe, because the center of mass momentum is always zero. Energy transfer in collisional activation and kinetic energy release during the dissociation of activated ions are deduced by applying the conservation of momentum and the conservation of energy to the process. The entire system is evaluated as a whole and velocities of the ion and neutral gas are stated as velocities relative to each other. The com kinetic energy of the colliding particles, not the laboratory kinetic energy of the ion, is the important parameter determining the nature of the activation step of the collision process. The description of the collision event and the frame transformation are often illustrated by means of two-dimensional *Newton diagrams*. These diagrams represent graphical representations of the ion and target gas velocities as well as the scattering angles in the center of mass reference frame. The treatment of these very useful diagrams is beyond the scope of this brief tutorial. The present authors suggest the excellent introduction provided by Cooks as a first reading.³² The total available energy for the transfer of kinetic energy to internal energy is the relative energy (E_{com}) and depends on the collision partners' masses. The following relationship relates the center of mass and laboratory collision energies:

$$E_{com} = \left(\frac{N}{m_p + N} \right) E_{lab}$$

where E_{lab} is the ion's kinetic energy and N and m_p represent the masses for the neutral target and precursor ion, respectively. The CID process is highly dependent on the relative masses of the two species. Conservation of energy means that if the relative translational energies of the colliding particles change by a certain amount this

energy must appear as internal energy, designated as the collision endothermicity, q (the amount of translational energy converted into internal energy). The maximum magnitude of q is seen in the case where the collision partners stick together, consisting of a totally inelastic collision. In this case, the final relative kinetic energy is zero. The value of q_{\max} is therefore equal to the initial center of mass energy. E_{com} represents the maximum amount of energy that can be converted into internal energy of the precursor ion. This energy, as seen in the equation above, increases with the target's mass, allowing more of the ion's kinetic energy to be converted into internal energy. Furthermore, E_{com} decreases as a function of $1/m_p$, so larger precursor ions have less internal energy available for fragmentation through the collision process.³³

During the collision process, collision partners approach and recede from each other while changes might occur at the molecular level. For the case of an elastic collision ($q = 0$), the kinetic energy of the system (and the internal states of the collision partners) is conserved. When $q > 0$, an inelastic process occurs with a decrease in kinetic energy (E_k) and a simultaneous increase in internal energy. Under superelastic conditions ($q < 0$), there is a net increase in E_k and decrease in internal energy. Collision induced activation of polyatomic ions is an example of an inelastic collision. Collisional activation mechanisms have been extensively studied for diatomic ions with neutral target atoms,³⁴ but are still not well defined for polyatomic ions. On the other hand the subsequent dissociation of activated ions is adequately explained by RRKM (or less well by the QET).³² The overall CID process is assumed to occur by a two-step mechanism, where the excitation of the precursors and their fragmentations are separated in time since the activation time for fast-moving ions is generally orders of magnitude faster than the dissociation time:



The second part of this mechanism is, of course, a unimolecular dissociation of an excited ion, and explains why QET can be used to rationalize CID spectra. Fragmentation of a precursor ion can occur if the collision energy is sufficiently high that the ion is excited beyond its threshold for dissociation. There exists, however, an amount of extra energy needed above and beyond that of the threshold energy, viz. the *kinetic shift*, for fragmentation to occur on the time-scale allotted by the experiment. The shorter the time scale of activation, the higher the kinetic shift necessary to observe fragments.

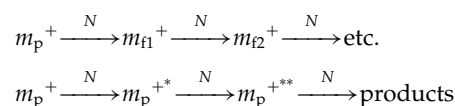
All CID processes occurring routinely can be separated into one of two categories based primarily on the translational energy of the precursor ion. For organic ions of moderate mass (several hundred daltons), *low-energy collisions*, common in quadrupole and ion trap instruments, occur in the 1–100 eV range of collision energy, and *high-energy collisions*, seen in sector and TOF/TOF instruments, are in the kiloelectronvolt range. Intermediate collision energies (100–1000 eV) do not occur in commonly used tandem mass spectrometers. There are important differences in the

resulting CID spectra under low and high collision energy conditions.

Low-energy collisions

In considering low-energy collisions, we deal in the range of 1–100 eV of laboratory collision energy, which is mostly observed in triple quadrupoles (QqQ) and trapping devices, such as quadrupole ion traps (IT) and Fourier-transform ion cyclotron resonance (FTICR) instruments. In a QqQ instrument, the collision cell is the second quadrupole (q_2) in the series and is operated in r.f.-only mode, allowing the ions to be focused. The collision cell is filled with a neutral inert gas, usually N_2 or Ar, and ion activation is achieved most often by multiple collisions.

In addition to the nature of the collision gas, the pressure in the collision cell is of significant importance. At higher gas pressures, both the number of ions undergoing collisions and the probability for an individual ion to collide several times with the target gas molecules increases.³³ Furthermore, the product ions formed by dissociation of the precursor ion can be further activated by subsequent collisions and then also dissociate at higher gas pressures. Busch *et al.*³³ describe these two limiting scenarios contributing to the CID spectrum:



The first reaction describes the CID of the precursor, followed by subsequent dissociation of activated product ions. The second reaction illustrates the stepwise activation of the precursor ion prior to dissociation. Both reactions lead to an increase in the total internal energy of the precursor ions. At higher gas pressure and collision probabilities, the collision energy deposition function resembles that of a Boltzmann distribution at elevated temperatures.²⁹ As pointed out by Busch *et al.*,³³ increasing the collision gas pressure is a convenient means of increasing the degree of dissociation of higher mass ions (for which E_{com} values are low) and ions that are particularly stable.

The probability of interaction, known as the collision cross section, is given by

$$\frac{I_0}{I} = e^{-n\sigma l}$$

where I_0 and I are beam intensities, n is the number of gas molecules, σ is the collision cross section and l is length of collision cell; σ is commonly expressed in \AA^2 per atom or cm^2 per atom. For CID, the cross-section is generally 10^{-14} – 10^{-17} cm^2 .

In a quadrupole ion trap, the precursor ions are isolated and accelerated by 'on-resonance' excitation causing collisions to occur and product ions are detected by subsequent ejection from the trap. In on-resonance excitation, the isolated precursor ion is excited by applying a small (tickle) a.c. potential across the end-caps, corresponding to the secular frequency of the ion. Ion activation times of the order of tens of milliseconds can be used without significant ion losses, therefore multiple collisions can occur

during the excitation period. Because of this relatively long time-scale, this excitation technique falls into the category of so-called 'slow heating' processes.³⁵ For a slow heating process, excitation in an ion trap is still fairly fast, owing to the high pressure of helium present in the trap (~1 mTorr). There are other slow heating methods, such as 'sustained off-resonance irradiation' (SORI, see next paragraph) or blackbody infrared radiative radiation (BIRD, see later) with much longer excitation periods.

As is the case for quadrupole ion traps, in FTICR instruments isolation and excitation take place in the same confined space, where the ions are trapped for a specific time in a combined magnetic and electrostatic field. On-resonance excitation in the FTICR cell can be achieved by using a short (hundreds of μs) high-amplitude a.c. signal at the natural cyclotron frequency of the precursor ion. This procedure excites the precursor ion rapidly via multiple collisions and deposits a large amount of energy in the ion. The short irradiation time is necessary to minimize precursor ion losses in the on-resonance experiment. However off-resonance excitation, the SORI technique, is usually applied for collisional activation of precursor ions in FTICR instruments. In SORI, the precursor ion is excited at a frequency slightly higher than the natural cyclotron frequency. In that way, ions undergo multiple acceleration/deceleration cycles as they repeatedly increase and decrease their orbit radii in the FTICR cell before dissociation takes place. As the ion translational energy is small compared with on-resonance excitation, much longer activation times can be used without ion loss, often hundreds of milliseconds, sometimes up to seconds,³⁵ and a larger number of collisions take place. Consequently, the ion sequentially absorbs more and more collision energy until the collision threshold is reached. As a result, slow, low-energy rearrangement reactions are favored.³⁶

For low collision energies, excitation is mostly vibrational, since the interaction time is of the order of $\sim 10^{-13}$ – 10^{-14} s, coinciding with a bond's vibration period.³⁷ However, molecular beam measurements of energy transfer/disposal in CID processes have shown that many of the previously held rationalizations about energy transfer mechanisms, e.g. high-energy collisions, involve electronic excitation whereas low-energy collisions involve vibrational excitation, are not always valid. For example, the common generalization that low-energy collisions proceed via vibrational excitation is clearly contradicted by experiments which measure energy transfer quantitatively.²⁹

The mass of the neutral target has a more important role for low-energy CID. More energy is transferred with heavier targets. Even though the average energy deposited per collision may be lower than in high-energy CID, product ion yields are very high, especially since multiple collisions are allowed by the gas pressure and length of the collision cell in a QqQ or the time allotted for CID in ion traps.

In the case of a triple quadrupole instrument, just as in the case already discussed of sector mass spectrometers, several scan modes exist although they are easier to implement using a triple quadrupole. The most common scan is the *product ion scan*, where a specific precursor is selected in Q_1 , fragmented in q_2 and the products are subsequently determined in Q_3 . A second scan is the *precursor ion scan*, which is essentially the reverse of the *product ion scan*. The third quadrupole is set to select a specific product ion formed in q_2 and the first quadrupole is scanned for all precursor ions forming the chosen fragment.

An important use for precursor ion scans is seen in the pharmaceutical industry. This experiment is convenient for identifying drug metabolites having similar fragmentation behavior and, hence, producing common fragment ions. The example in Fig. 7 shows two metabolites of ciprofloxacin that

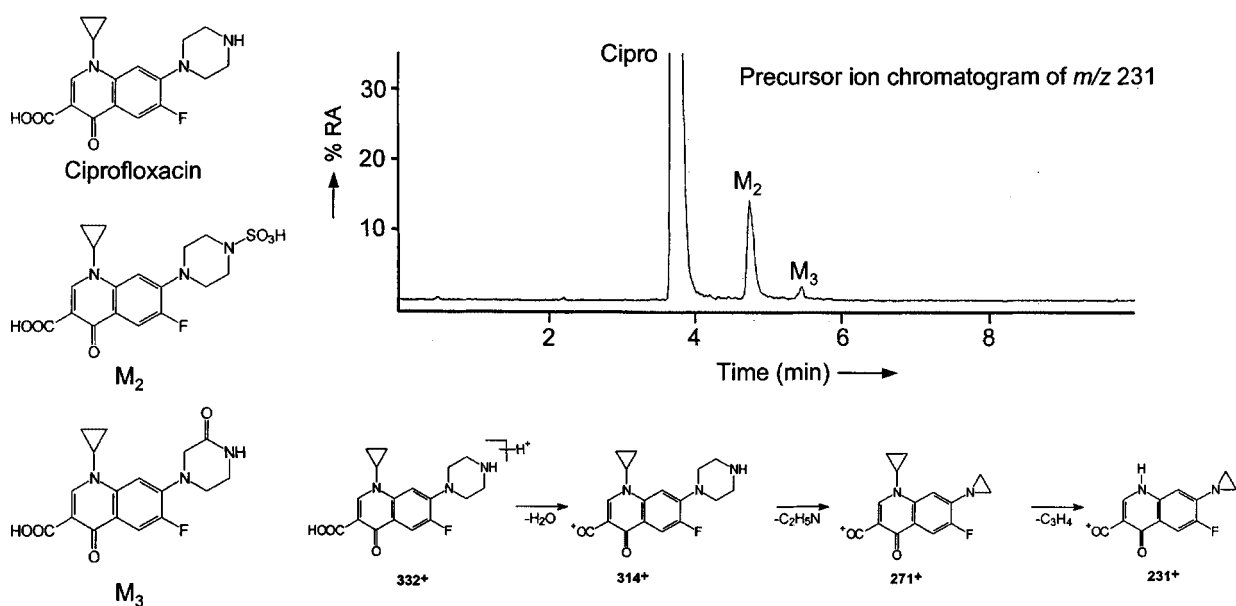


Figure 7. Example of a *precursor ion scan* experiment for the determination of ciprofloxacin and two of its known metabolites. The fragmentation pathway is outlined for the formation of product ion m/z 231 for protonated ciprofloxacin (m/z 332). The above chromatogram reveals two metabolites formed in human urine. From Ref. 38. (Chromatographic trace reprinted with permission, © 1997 American Chemical Society).

are detected in human urine using a *precursor ion scan* of a common fragment at m/z 231.³⁸ This experiment yields a chromatogram with all species exhibiting this structurally relevant product ion after CID. A third experiment is the *neutral loss scan* which is also achieved in this instrument with relative ease. Neutral loss scans are routinely used for rapid diagnosis in neonatal screening of metabolic diseases, including maple syrup urine disease and homocystinuria. Figure 8 exhibits the *neutral loss scan* experiment used for the detection of homocystinuria. In this assay, all amino acids are first derivatized to their butyl ester derivatives and subsequently detected by a common loss of the neutral butyl ester. Figure 8(A) is a *product ion scan* for the butyl ester derivative of methionine (m/z 206) revealing a strong fragment ion at m/z 104 (neutral loss of 102 Da). Comparison of neutral loss scans from a control blood sample and one from a neonatal patient with homocystinuria detects the disease by determining the ratio of methionine to the summed contribution of leucine and isoleucine. The disease state, as seen from comparing the spectra in Fig. 8(B) and (C), has a much elevated ratio.³⁹

Interestingly, multiple stages of CID can be performed in IT instruments, although the experiment is restricted to the

product ion scan. This is advantageous for the elucidation of fragmentation pathways and for the identification of molecular structures of ions. Several hybrid geometries have recently been introduced with specific advantages, including the quadrupole-linear ion trap (QqLIT) and the quadrupole-time of flight (QqTOF) instruments. The former allows triple quadrupole scan types as well as MS³ capabilities in the linear ion trap,⁴⁰ while the latter yields product ion spectra with greater resolution and thus higher mass accuracies for product ions.⁴¹ Some commercial instruments can even achieve low-energy CID in an r.f.-only quadrupole with a hybrid Qq-FTICR instrument.⁴² Additionally, a recently introduced FTICR instrument employs a linear ion trap for multiple stages of front end CID.⁴³

High-energy collisions

Collisional activation occurs in the keV range in sector and TOF instruments, when precursor ions have very high translational energy. In both types of instrument, a collision cell is placed between the two mass analyzers. The precursor ion beam, having a kinetic energy of a few keV, can enter the collision cell, usually causing single collisions before mass analysis of the product ions. The same linked scans as previously described in the metastable

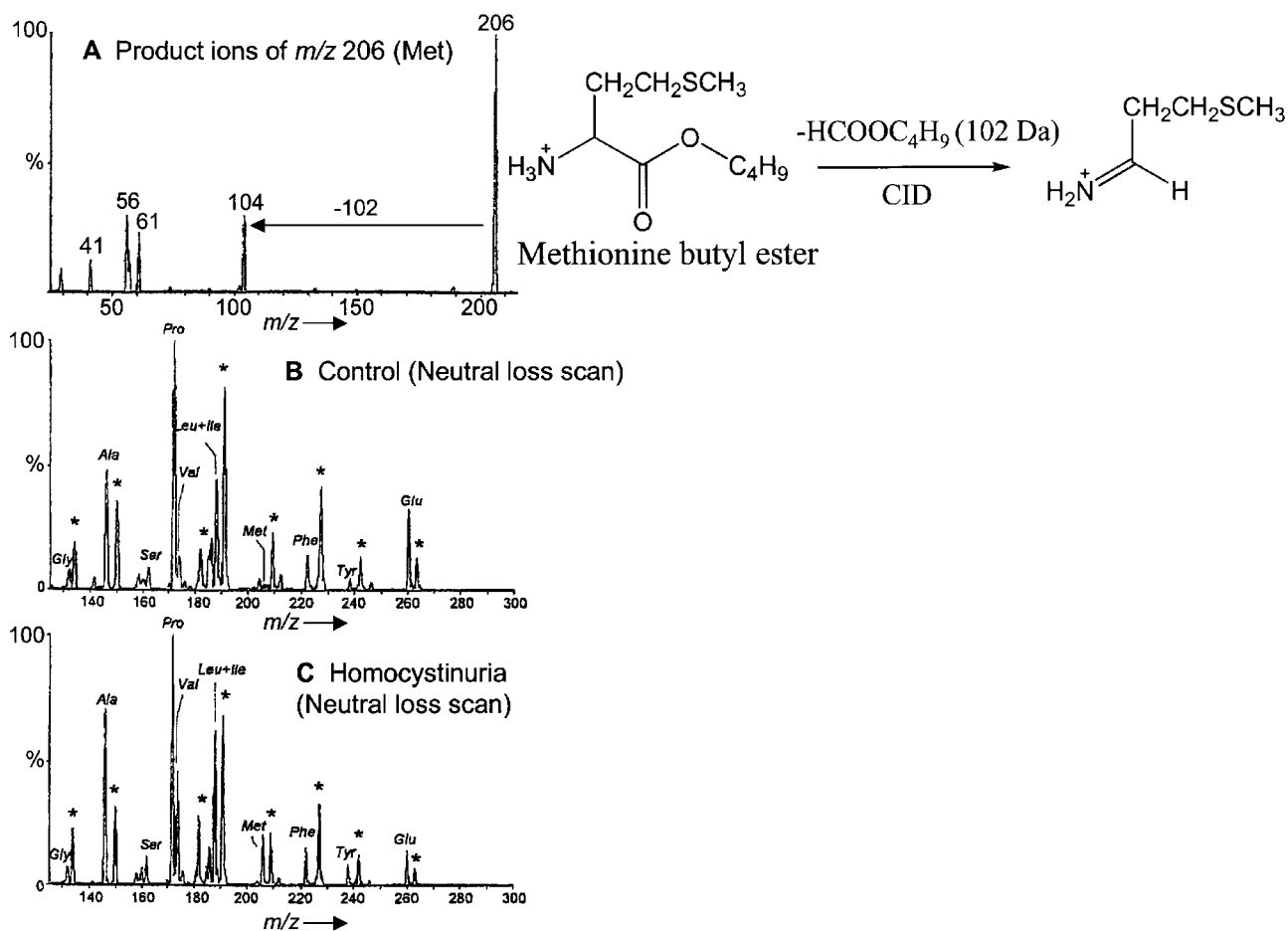


Figure 8. An example of a *neutral loss scan* is shown for the determination of homocystinuria (metabolic disease) in newborns. (A) *Product ion scan* of methionine butyl ester derivative. Scanning for a common neutral loss of 102 (butyl ester) is used to quantify all amino acids, which are initially derivatized to their butyl ester derivatives. The ratios of methionine to the summed contribution of leucine and isoleucine are compared for control (B) and disease-state (C) samples for detection of homocystinuria. Asterisks denote spiked deuterated amino acids used as internal standards in the assay. From Ref. 33 (reproduced by courtesy of AACCC).

ion decomposition section can also be employed for the analysis of CID products in sector instruments. Four-sector mass spectrometers (a pair of electric sector/magnetic sector combinations) allow high resolution of both precursor and product ions; however, these instruments suffer from poor sensitivity due to transmission losses. PSD products in TOF instruments can be increased by either performing the experiments under low-vacuum conditions¹⁶ and therefore causing collisions with residual gas to occur in the flight tube or by placing a collision cell immediately after the ion source in a TOF instrument.⁴⁴ A tandem TOF instrument has a high-energy collision cell placed between two TOF mass analysers, with good resolving power in both stages of mass analysis.⁴⁵ High-energy CID generally employs helium as the target gas, but collision yield may be increased by using a heavier gas, such as Ar or Xe.

Ion excitation is mainly electronic at high kinetic energies.⁴⁶ It is, however, noteworthy that vibrational and rotational energies can also play an important role in the excitation.⁴⁷ The conversion of kinetic energy to internal energy is most efficient when the interaction time of the collision coincides with the period of the internal mode undergoing excitation.⁴⁸ If activation causes an initial vertical electronic transition, redistribution of the energy acquired into vibrational modes of the precursor ion's ground electronic state may follow and be the reason for a bond cleavage. The randomization of energy occurs by radiationless transitions within the excited precursor ion with consequent CID.

The two energy regimes possible for CID often yield different products. This fact can be used to our advantage, since structurally important fragments can be formed in both techniques. For unimolecular dissociations, higher ion energies are required for direct bond cleavages than for rearrangement reactions.³¹ The case of fragmentation of ketone molecular ions illustrates this scenario. Two possible fragmentation routes are the α -cleavage (direct bond cleavage) and the McLafferty rearrangement, the contribution of the latter being increased as energy is decreased.¹⁰ It has also been reported that high-energy CID imparts a wide range of energies to the precursors, including much higher activation energies.⁴⁹ A detailed study on the internal energy distributions on ions has been provided by Wysocki *et al.*,⁴⁹ which includes a nice example illustrating this difference. Figure 9 gives an example from this paper with the different $P(E)$ curves resulting from low and high-energy collision experiments for the phenanthrene molecular ion.⁴⁹ Threshold energies for several reactions are not achieved in the low-energy collision regime, resulting in many fewer fragment ions. It can be assumed that high-energy CID allows an increase in direct bond cleavage products in the tandem mass spectra as compared with the low-energy case. There is a trend towards higher energy products, resulting mostly from direct bond cleavages, as the collision energy is increased. Another interesting example is noted for the fragmentation spectra of peptides. Specific fragmentation nomenclature has been developed for peptides, based on which bonds are cleaved in the dissociation process.⁵⁰ The low- and high-energy CID spectra

for the decapeptide ACTH are shown in Fig. 10.⁵¹ We see that high-energy collisions in a four-sector instrument yield primarily v and w ions, while the low-energy CID spectra in a triple quadrupole exhibits mostly b and y ions. The fragmentation mechanisms^{15,52} for the formation of these products explain their abundance in the two types of spectra. High-energy CID spectra usually show increased side-chain fragmentation in addition to richer tandem mass spectra than in the case of low-energy activation.⁵³ Although CID remains the most common activation method in mass spectrometry, there has been a recent emergence of new activation techniques, each with their own advantages and applications, one of which is surface-induced dissociation (SID).

SURFACE-INDUCED DISSOCIATION

This method of activation represents a procedure analogous to CID, except that a solid surface is used as a collision target instead of an inert gas molecule. Simply put, kinetic energy of the projectile ion is transferred into potential energy upon collision with a solid surface, with resulting activation of the precursor ion and subsequent dissociation. SID was first developed in the 1970s and most of the pioneering studies were performed in Cooks' laboratory at Purdue University.^{54,55} Since its inception, SID has been studied by several other research groups also, including those of McLafferty,^{56,57} Wysocki^{58–60} and Futrell.^{61–63} The main idea behind this activation method stems from the fact that energy transfer in CID is limited by the energy available in the center-of-mass reference frame (E_{com}), which is dependent on the mass of the target gas (see above). By increasing the mass of the target, E_{com} becomes larger and thus energy transfer can be improved. Assuming (as an extreme) that collisions occur with the entire surface instead of individual surface molecules, the mass of this colliding species is effectively infinite. Energy conversion, in theory, should therefore be much more efficient in SID. There are instances, though, where terminal groups on the surface appear to be primarily responsible for energy conversion.⁶⁴

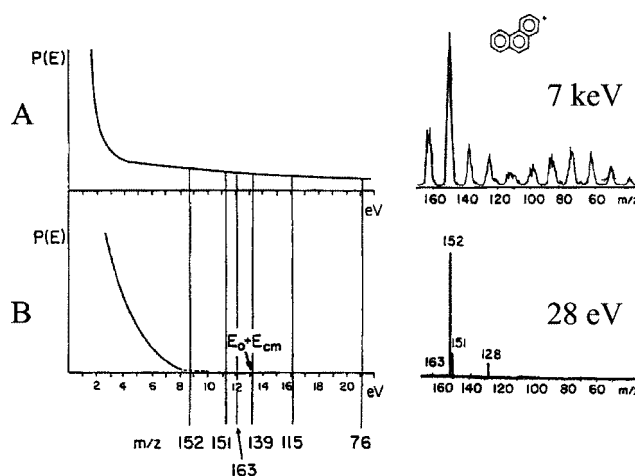


Figure 9. $P(E)$ distribution curves and product ion spectra for high-energy (A) and low-energy (B) CID of phenanthrene ions. Activation energies of several product ions are noted. From Ref. 50 (reproduced by courtesy of Elsevier Science).

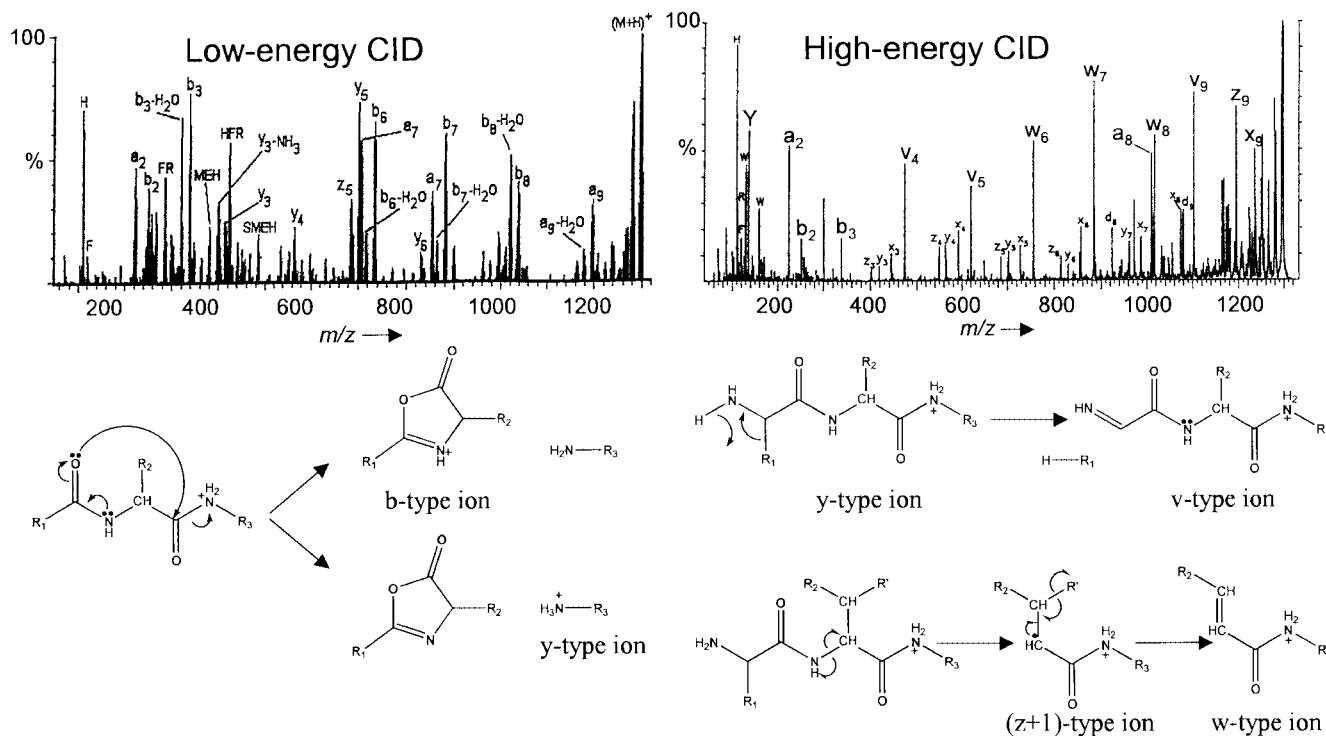


Figure 10. Different fragmentations pathways for protonated peptides are shown under low- and high-energy CID conditions. The high-energy CID of ATCH decapeptide produces mainly v and w ions, whereas low-energy CID yields b and y ions. Both methods can be used to gain complementary information. This can therefore improve sequence coverage and reliability of data. From Ref. 51 (reproduced by courtesy of Elsevier Science). Fragmentation shown according to Refs 14 and 45.

In this case, the center-of-mass collision energy is calculated using the mass of these groups.

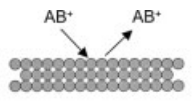
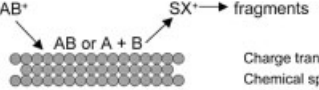
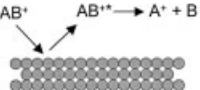
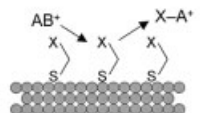
Cooks and co-workers have arbitrarily classified the collision events at surfaces according to the collision energy of the impacting projectile (neutral molecules, ions, atoms).⁶⁵ SID reactions fall in the 'hyperthermal' regime (energies between 1 and 100 eV). In this regime, the center-of-mass collision energies are of the order of or greater than chemical bond energies and they allow bond cleavages in addition to rearrangement reactions. Other energy regimes not covered in this tutorial include very small collision energies (meV to a few eV; 'thermal range') and keV to MeV collisions. In these regimes, usually no specific information on the chemical nature of the impacting ion is obtained. Hence hyperthermal ions are the primary subject of this section. Hyperthermal ions can scatter on a surface in an elastic, inelastic or chemically reactive fashion. Elastic scattering events can lead to 'soft landing' of ions by removing translational energy from the ions and depositing them on the surface.⁶⁶ Inelastic and reactive scattering events, however, are the most common processes observed at the collision energies typically implemented in SID, where the reactive scattering reactions are undesired side reactions leading to reduced efficiency and sensitivity in SID (see below). Table 2 illustrates the major hyperthermal reactions induced by surface collisions with increasing collision energies.

In general, similar products are observed in SID and CID and the mechanism of activation for SID is therefore rationalized as a two-step process. Initially, the incident ion inelastically collides with the solid surface, forming an

internally excited ion, which then undergoes unimolecular dissociations. The interaction time with the surface is of the order of 10^{-12} s, a short period compared with the dissociation time required for polyatomic ions (maximum dissociation constants: 10^{10} – 10^{12} s⁻¹).⁵⁵ The SID experiment is believed to involve collisional activation at the surface followed by delayed gas-phase dissociation of the scattered projectile ion. However, there is evidence for another process based on a sudden increase in the number of observable peaks (from 2–5 to >50) with change in collision energy from 10 to 30 eV. It is suggested that shattering of the projectile ion occurs at the surface at these higher collision energies⁶⁷ and this results in fragment ions which have the same kinetic energy since they all originate at the surface. By contrast, dissociations taking place in the gas phase after the precursor ion has left the surface have similar velocities. For example, Schulz *et al.*⁶⁸ found the same velocity distribution for small peptide fragment ions after collision with a hexanethiolate self-assembled monolayer (SAM, see below), indicating gas-phase dissociation after the precursor ions had already left the surface.

The internal energy distributions of excited ions for SID are relatively narrow,⁶⁹ therefore this activation method offers an advantage over CID, where the internal energy of ions is not as narrow. In general, all incident ions directly collide with the surface, whereas in CID most collisions are glancing. Consequently, the energy transferred can be readily varied with changing the impact energy. This can be useful for identifying the relative energies needed for specific fragmentation pathways to occur. The center-of-mass

Table 2. Elementary processes in ion–surface interactions (adapted from Ref. 66)

	Elastic scattering Quasi-elastic scattering	$AB^+ + SX \rightarrow AB^+ + SX$ $AB^+ + SX \rightarrow AB^{2+} + SX$
	Charge transfer Chemical sputtering	$AB^+ + SX \rightarrow SA + SB + SX^+$ $AB^+ + SX \rightarrow AB + SX^+ \rightarrow S^+/X^+$
	Surface-induced dissociation	$AB^+ + SX \rightarrow AB^{2+} + SX \rightarrow A^+ + B + SX$
	Ion-surface reactions	$AB^+ + SX \rightarrow AX^+ + SB$

collision energy for SID is difficult to determine, but if we assume the mass of the target, N , to represent the mass of the collection of atoms in the surface, the $N/(N + m_p)$ ratio would essentially be unity, and E_{com} would equal E_{lab} . However, as explained above, this assumption is not always possible, and a specific mass should then be considered for the colliding neutral target.⁶⁴ Some simulation experiments, such as the Hase model,⁷⁰ however, have shed some light on this subject. It has been shown that several experimental factors (such as surface composition, projectile structure, collision energy, incidence angle) influence the amount of energy transferred into internal energy of the ion.⁷⁰

Since SID yields a relatively narrow range of internal energies, it has a potential application in isomer distinction when comparing relative intensities in energy-resolved mass spectrometry.⁵⁸ Conversely, in the case of CID, two stable ions with a low interconversion barrier can give similar tandem mass spectra. SID spectra have been shown to be reproducible with good signal-to-noise ratios. Furthermore, the reaction region does not need additional pumping stages, since no extra gas is introduced as in CID. The solid surface is directly in the path of the incident beam, yielding 100% interaction efficiency; however, this does not necessarily imply higher overall collision yields than CID.

The advantages of SID over CID are often diluted when a metal surface is selected due to the presence of several competing processes, viz. neutralization, chemical sputtering from the surface and ion–surface complex formation reactions (Table 2).^{65,71} Neutralization of the incident ion beam is especially apparent when the metal surface, or the adsorbate present on the surface, has a low ionization potential, thus the charge can easily be transferred from the ion to the surface. Resulting surface ions can also end up with additional internal energy from the collision and dissociate into products, a phenomenon known as chemical sputtering. Ion–surface reactions, such as abstraction of a hydrogen atom or a methyl group, are common when surfaces bear adsorbates. At the operating pressures in the SID reaction region, the surface is usually covered with impurities, mostly derived from residual pump oil.

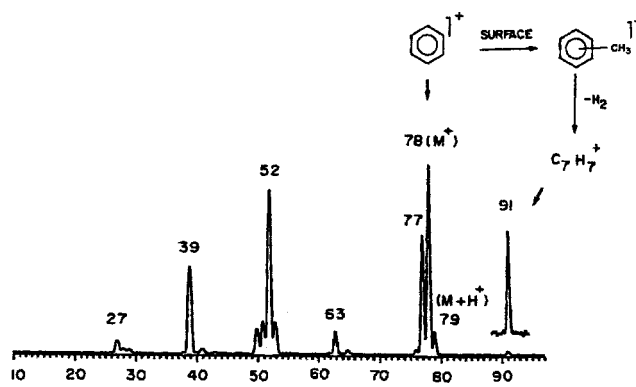


Figure 11. An SID spectrum is shown for the benzene molecular ion. Ion–surface reactions are apparent by the presence at m/z 91, corresponding to the stable tropylium ion. This product is formed by initial methyl abstraction from the adsorbate present on the surface target, followed by the loss of a hydrogen molecule (H_2). Note also that m/z 78 corresponds to the protonated ion, formed by hydrogen abstraction from the surface, another common ion–surface reaction seen in SID. From Ref. 47 (reproduced by courtesy of John Wiley and Sons).

In general, even electron species do not undergo ion–surface reactions, although we often see molecular ions ($M^{+\bullet}$) abstracting a hydrogen resulting in an $[M + H]^+$ species,⁷² which can subsequently dissociate. Hydrocarbon adsorbates present on these metal surfaces are the suggested source for the abstracted hydrogen. An interesting example is also seen with SID of the benzene molecular ion. The precursor can abstract a methyl group from the surface, followed by loss of H_2 forming the highly stable tropylium ion.⁷³ The SID spectrum of the benzene molecular ion is illustrated in Fig. 11.⁵⁵ It has also been reported that changing the nature of the adsorbate can decrease the extent of neutralization of the ion beam, which has been estimated to represent up to 90% of the precursor ions lost with most metal surfaces.⁵⁵ Recently, surfaces for SID have been modified by using SAMs.^{74,75} The fluorinated SAM surfaces consist of a fluorinated self-assembled monolayer of thiolate, which has a high ionization

potential and, hence, does not promote charge exchange between the ion and the surface. These surfaces have been studied extensively and are mostly resistant to surface damage.⁶⁰

Several different instruments have been employed for SID of polyatomic ions; however, important modifications to the mass spectrometer are usually necessary. An in-line BqQ hybrid has been modified to allow the large scattering angles needed for the study of ion–surface reactions.⁵⁵ Special ion optics are used for the deceleration of the ion beam and extraction of the products for analysis by the quadrupole. Triple quadrupoles can also be altered to accommodate SID.⁷⁶ The second quadrupole is operated in r.f.-only mode and serves as an ion guide in front of the target. Q₃ is placed at right-angles to the other two quadrupoles. This geometry allows the introduction of gas into q₂ for consecutive gas-phase and surface collisions. A TOF/TOF instrument with a 90° scattering angle and a solid surface placed between the two analyzers can also be used to perform SID.^{77,78} Since the resulting fragments have a range of kinetic energies, the beam must be accelerated from the surface to achieve good mass resolution. However, low resolution of product ions still remains a problem.⁷⁹ This instrument allows very rapid SID data acquisition and can access high collision energies (up to 750 eV). A reflectron TOF can be used for ion–surface collisions by placing the surface target at the end of the reflector.^{80–82} SID has also been performed in FTICR^{56,57,83,84} and ion trap⁸⁵ instruments, by first trapping the ions and subsequently accelerating them into either the walls of the trap or a probe placed at one end of the FTICR cell. SID is especially advantageous for FTICR-MS, given that CID in these instruments requires the introduction of gas, which has a negative effect on mass resolution. More effective dissociation can also be seen in trapping instruments since multiple stages of SID can be performed. SID in an FTICR instrument has been reported to be especially effective for the dissociation of large peptides.^{56,86} Unfortunately, most of these instruments suffer from poor transmission of the emerging ion beams. Also, instrument modifications often need to be made to accommodate the non-linear collision geometry necessary for SID. Several recent advances in optical and surface optimization have increased the overall collision yields of SID, yet improved efficiency is still needed. This activation method remains a very promising technique, especially for high-mass ions, such as peptides and proteins, with relatively high dissociation thresholds. SID, however, still awaits incorporation into a commercial instrument. Another method that has interesting applications, especially for proteomics research, is electron capture dissociation (ECD), which represents the next topic of discussion.

ELECTRON CAPTURE DISSOCIATION

In this section, we introduce the technique of electron capture dissociation (ECD), which was developed by McLafferty's group in 1998.⁸⁷ Briefly, it involves the capture of low-energy electrons by multiply charged ions, with charge-state reduction and subsequent fragmentation. This method was originally developed for the analysis of multiply

charged peptides and proteins by electrospray ionization. An excellent review of the history and mechanism of ECD was presented by Zubarev *et al.* in 2002.⁸⁸ The ECD method for ion activation is the result of several important observations from ion–electron reactions, which are all clearly described in Zubarev *et al.*'s review. Specifically, the study of dissociative recombination (DR) correlates well with ECD.⁸⁸ DR involves the fragmentation of gaseous positive ions following electron capture, where the excited neutral then dissociates into two neutrals (one radical and one even-electron species). Stabilization of the captured electron is faster than electron emission, which is usually on the time-scale of 10⁻¹⁴ s. Bond dissociation, therefore, occurs faster than a typical bond vibration. The main difference in the case of ECD is the charge-state of the precursor ions and the resulting species. Also, the process is non-ergodic. Removing the unpaired electron from this multiply charged ion should require 5–7 eV of energy; conversely, the electron addition that formed this hypervalent species should also add 5–7 eV of recombination energy.⁸⁹ Randomization of this energy over the thousands of degrees of freedom of a large protein ion would result in only millivolts of excitation per bond. However, with a non-ergodic process, bond cleavage occurs by this addition of energy before it is randomized away from the reaction site. The major advantage of ECD is the ability to cause dissociation in very large biomolecules (~40 kDa) at many sites, where other methods of dissociation are less effective.

ECD usually employs a tungsten filament forming a beam of very low-energy electrons (<0.2 eV) for activation of the precursor ion. A low-energy electron source based on an indirectly heated dispenser cathode, however, has been shown to cause significant improvement for the process and greatly decreases the corresponding time needed for ECD experiments.⁹⁰ FTICR-MS is ideal for the application of ECD⁸⁹ and, accordingly, all commercial FTICR instruments currently provide this technique. Since the electron beam is fairly narrow compared with the ion packets in the ICR cell, long interaction times (up to minutes) are needed for good fragment ion abundances.⁹¹ As a consequence, not all ions are activated instantaneously, even though the ECD activation process itself is very short (<10⁻¹⁴ s).⁹² The FTICR cell traps the ions by simultaneously applying strong magnetic and weak electrostatic fields, while having virtually no influence on the kinetic energy of the electrons during their interaction with the precursor ions.⁹¹ Unfortunately, it remains difficult to perform ECD in a quadrupole ion trap instrument, where the ions are trapped by strong r.f. potentials applied to the ring electrode, affecting the electrons' movement in the trap.

Charge neutralization occurs when a singly charged ion undergoes electron capture and the resulting neutral, obviously, cannot be detected by the mass spectrometer. ECD is, as a result, only applicable to multiply charged cationic species. The mechanism of dissociation involves the fragmentation of an odd-electron ion, resulting from electron capture on to an even-electron species. The dissociation of the ion is restricted to specific protonation (or cationic) sites where the electron is captured. As a result, bond cleavages are governed by radical ion chemistry.¹⁰ The

radical species resulting from electron capture has very different bond strengths to the original precursor and therefore the fragmentation pathways can differ greatly.

Electron capture depends strongly on electron energy, whereby the efficiency of the process increases 1000-fold by decreasing the energy from 1 to <0.2 eV.⁹³ There is also efficient electron capture at higher energies, with a maximum at ~ 7 eV,⁹⁴ and this is referred to as hot-ECD (HECD). This regime is still much less efficient, however, than regular ECD (<0.2 eV electrons). The much larger electron current produced from the indirectly heated cathode electron source can cause HECD to have similar efficiency and capture cross-section to ECD. Other electron energies also cause dissociation reactions, but these have very different mechanisms, including electronic-excitation dissociation (EED) and electron-detachment dissociation (EDD).⁹¹

If we discuss the mechanism of ECD in a little more detail, the electron is not necessarily captured directly at the charge site. The electron can land far from the cationic site with subsequent electron transfer to the highest charge density site. The intramolecular potential difference, which causes this secondary electron transfer, is especially apparent in multiply charged metal ion complexes. These metal ions, such as Fe^{3+} or Zn^{2+} , serve as an electron sink and we accordingly see much less fragmentations within a certain region close to the metal.⁹³ The landing of an electron on a multiply charged precursor ion creates a hypervalent (hydrogen-excess) unstable species. Groups with high affinity for the hot hydrogen atom, such as carbonyl or disulfide bonds, are principal sites for capture. The exothermicity of charge reduction and H^\bullet capture leads to bond cleavage initiated at the radical site.

ECD has been described as a non-ergodic process,⁹⁵ where energy is not redistributed over the whole molecule and weakest bonds are not preferentially broken following ion activation. This characteristic behavior is illustrated very well by comparing the fragmentation reactions of multiply charged peptides for ECD and the vibrational excitation (ergodic) methods. Ion activation for all other methods is based on the vibrational excitation with rapid redistribution throughout the whole precursor ion prior to dissociation. Fragmentation pathways can be rationalized by the statistical quasi-equilibrium and RRKM theories and depend only on the amount of energy deposited, not the method of ion activation. Ergodic activation methods, such as CID and IRMPD (see below), result in cleavage sites at the most vulnerable bonds, such as peptide bonds, through rearrangement reactions. Accordingly, tandem mass spectra look very similar for all other activation methods. ECD, however, is assumed to occur much faster than 10^{-12} s, permitting the occurrence of direct bond cleavages only. As a result, it has been reported that the strong backbone $\text{N}-\text{C}_\alpha$ bonds of peptides are cleaved, forming c' and z -type ions. Also, disulfide bonds, which are fairly stable under other ion activation conditions, are preferentially broken. An obvious advantage is the possibility of identifying sites of post-translational modifications, which remains especially difficult for the very labile γ -carboxyl, o -glycosyl and sulfate

linkages using other methods.⁹¹ In addition, even non-covalent interactions are stable under ECD conditions,⁹⁶ allowing specific sites of interactions to be studied in addition to gas-phase secondary and tertiary protein structure. The c' and z ions are also observed with HECD, but since we have excess energy, we often also see secondary fragments of the z ions, giving w ions through side-chain cleavages. These fragment ions are useful in distinguishing the isomeric leucine and isoleucine amino acids in a peptide sequence.⁹⁴ Additionally, cleavage of peptide bonds, yielding b - and y -type ions, can occur with HECD.⁹⁴ ECD has mostly been used in the field of proteomics since it often yields better sequence coverage than CID, making it very important for the identification of modification sites. It has also been applied to polymers,^{97,98} peptide nucleic acids⁹⁹ and oligonucleotides.¹⁰⁰ A good example illustrating the difference in fragmentation pathways between vibrational excitation methods and ECD is given in Fig. 12.¹⁰¹ The ECD and infrared multiphoton dissociation (IRMPD, see below) spectra of glycopeptides exhibit different product ions. There is extensive fragmentation of the labile sugar portions in IRMPD, whereas minimal fragmentation of the post-translational modification groups occurs with ECD. The latter technique is therefore very useful in the study of protein glycosylation and complementary information can be obtained by using it in combination with other activation methods. IRMPD is the next method to be explained, and is also employed in FTICR and other trapping instruments.

INFRARED MULTIPHOTON DISSOCIATION

The next activation method to be addressed is photodissociation. Ions can be excited and subsequently fragmented by the absorption of one or more photons. This type of activation of gaseous ions in a mass spectrometer has been performed with a range of photon energies, primarily by using lasers of different wavelengths. Historically, lasers emitting in the UV region, such as ArF excimer lasers (193 nm), and visible regions were used. Recently, there has been an increase in the use of IR lasers for photodissociation. These lasers are of low energies compared with UV lasers, where the absorption of only one photon provided enough energy to initiate dissociation of precursor ions. In IR, multiphoton processes are consequently needed to excite ions sufficiently for efficient fragmentation.

The chemistry of small molecules has been studied by IRMPD for a long time.^{102–104} The recent increase in applications for IRMPD as an activation technique in MS/MS is primarily due to the growth in popularity of trapping instruments, including quadrupole ion traps and Fourier transform ion cyclotron resonance mass spectrometers. IRMPD is ideally suited to these instruments, given their ability to store ions for long times. Typically, ions in the ion trap or the ICR cell are activated by a low-power (<100 W) continuous-wave CO_2 (10.6 μm) laser for a selected irradiance time (usually on the order of tens to hundreds of milliseconds), followed by the detection of the resulting product ions.

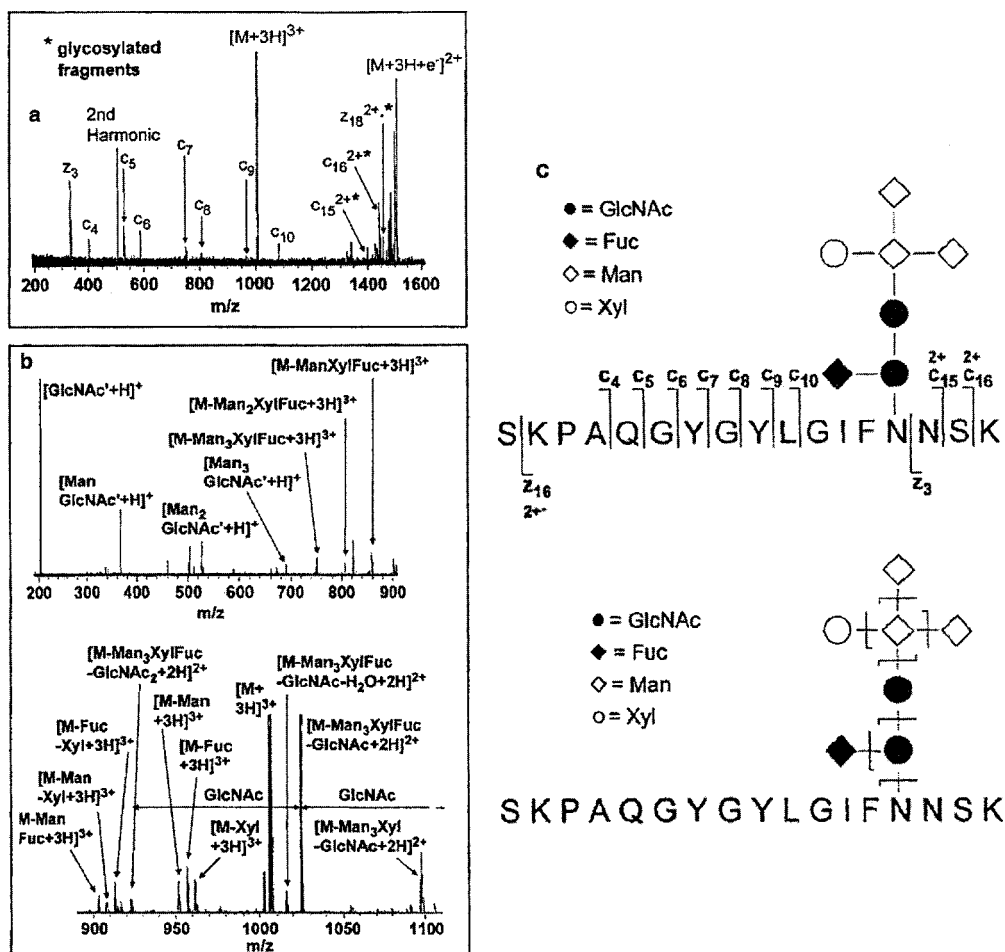
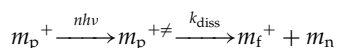


Figure 12. Comparison of ECD and IRMPD spectra for a triply charged *N*-glycosylated peptide of *m/z* 1005.5. Backbone amine cleavages (11 out of 15) are observed in the ECD spectra, yielding *c*-type ions with good sequence coverage, while glycan fragmentation predominates in the IRMPD spectra. Complementary information can be obtained by using both techniques for the characterization of glycosylated peptides. From Ref. 97 (reproduced with permission, © 2001 American Chemical Society).

Photodissociation can be generally viewed by the following mechanism:



where n describes the number of absorbed photons, $h\nu$ is the photon energy and k_{diss} is the rate constant for photodissociation. The mechanism of activation is assumed to be through the absorption of IR radiation by IR active modes present in the ion, followed by the rapid redistribution of energy over all the vibrational degrees of freedom. The outcome is a statistical internal energy distribution, similar to CID. The activation is stepwise, by subsequent absorption of photons, and dissociation occurs by low-energy pathways, often the lowest that is available. There are several important criteria for photodissociation to occur. The precursor ion must be able to absorb energy in the form of photons, producing excited states above the threshold of dissociation for the ion of interest. Competitive collisional and radiative cooling of ions also occurs, partially decreasing the energy gained by photon absorption and thus lowering the overall rate for dissociation. The energy gained by the absorption of photons must consequently overcome the energy lost by photon emission from the excited ions, as well as deactivation

by collisions. The presence of gas in the activation region (storage device) increases the chances for deactivation of the excited ions. In an FTICR instrument, this fact does not pose a problem since extremely low pressures are maintained in the cell. Conversely, the quadrupole ion trap has a constant amount of helium buffer gas present in the trapping region at all times to help narrow the kinetic energy distribution of the ions, so collisional deactivation can become an issue. A compromise is usually reached with a lower helium pressure than usual in the ion trap, as removing the helium altogether would cause peak resolution to suffer tremendously.

A very important advantage of IRMPD over CID in an ion trap comes from the fact that the trapping conditions, such as the r.f. voltages, do not need to be altered in the activation process. In a typical ion trap CID experiment, the precursor ion of interest is selectively accelerated by resonant excitation (see above). Multiple collisions and stepwise energy deposition occur, until an energy threshold is surpassed and dissociation takes place. The necessary conditions for CID in an IT cause an inherent low-mass cut-off for the detection of product ions, so low-mass fragments are not observed even if they are easily formed. A tradeoff must be made between the amount of internal energy available, which depends on the potential well depth ($\propto q_z$), and the

low-mass cut-off for product ions. Usually, CID conditions necessitate high q_z values. Photodissociation, however, can occur efficiently at very low q_z values.¹⁰⁵ IRMPD in ion traps allows for the storage of a wide m/z range of ions with less product ion mass discrimination. No fragments would be observable for CID under these trapping conditions.

The ion activation by photodissociation is rather non-selective, therefore all trapped ions are excited and secondary product ions can be observed. We therefore gain several new fragments compared with on-resonance or SORI CID (see above), as product ions derived from the precursor ion can be further excited into dissociative states. Keep in mind, though, that this outcome can also be disadvantageous if too many ions are formed and the resulting spectrum is a complicated collection of peaks. Moreover, the sequence of fragmentation pathways can easily be lost in such a situation. Fortunately, applying tailored excitation waveforms, such as 'stored waveform inverse Fourier transforms' (SWIFT),¹⁰⁶ may be used to eject specific product ions selectively from the trap. Fragment ions that disappear are concluded to be products of the ejected ions. This technique has been employed for IRMPD of macrolide antibiotics in a quadrupole ion trap.¹⁰⁴

The advantages of IRMPD are numerous. Particularly, the amount of available energy is well defined. In the case of a 10.6 μm CO₂ laser, the absorption of one photon corresponds to 0.117 eV of energy. The dissociation efficiency of this technique is good, given enough time for activation, and it can easily be implemented in routine analytical laboratories. Dissociation of precursor ions does not compete with scattering and ejection out of the trapping region. In the case of FTICR, gas does not need to be added to the cell. However, the cost of this technique is high and direct fragmentation pathways are often not easily determined, as in CID.

Interestingly, Hofstadler and co-workers^{107,108} have performed IRMPD in an r.f.-only hexapole, acting as an external ion storage device, prior to FTICR detection. The hexapole represents a narrower path than the FTICR cell, so the laser beam is able to interact with a larger number of ions having increased excitation efficiency. These studies exhibit IRMPD in a device other than the mass analyzer and show promise for the use of IRMPD with other instruments, such as TOFs. Recent studies have generally focused on the analysis of biomolecules by MS/MS and IRMPD has proven useful in these applications. The technique has been successfully employed for proteins,^{109,110} oligosaccharides,¹¹¹ oligonucleotides^{112,113} and pharmaceuticals.^{105,114,115} IRMPD has been combined with ECD^{116,117} and with collisional activation.¹¹⁸ It has been reported that these combinations can yield richer fragmentation spectra than the individual activation methods alone. The last ion activation technique discussed is the thermal dissociation of precursor ions in trapping instruments by blackbody infrared radiative dissociation (BIRD).

BLACKBODY INFRARED RADIATIVE DISSOCIATION (BIRD)

In an FTICR mass spectrometer, activation of ions can be accomplished by heating the ICR cell. Heating causes

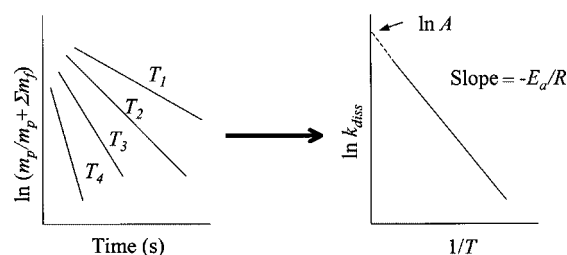


Figure 13. Procedure for deducing kinetic constants from BIRD data. Fragmentation of the precursor ion is followed at different activation times. If $\ln(m_p/m_p + \Sigma m_f)$ vs activation time is plotted for several reaction temperatures, first-order dissociation rate constants can be found from the slope. A second plot can be constructed for $\ln k_{\text{diss}}$ vs $1/T$. Both activation energy and the Arrhenius constant (a measure of the entropy of the dissociation reaction) can be calculated for the slope and the intercept of the resulting graph, respectively.

the trapped ions to absorb blackbody photons emitted from the walls of the cell. Dissociation occurs with no other source of excitation, such as collisional activation, owing to the extremely low pressures in this instrument. This is known as blackbody infrared radiative dissociation (BIRD) and represents a new method for the dissociation of large ions.¹¹⁹ There are two essential requirements for the blackbody mechanism; first, that the ambient pressure is low enough ($<10^{-6}$ Torr) so that IR photon absorption and emission compete significantly with collisional energy exchange; second, that the time-scale of observation of the dissociating molecules is long enough (of the order of seconds) for any significant degree of dissociation. An unreactive bath gas can also be added into the cell in order to remove excess ion velocity from the precursor ion population. In the case of large ions (>50 atoms), the rate of energy transfer of absorption and emission of photons can be greater than the rate of dissociation. A Boltzmann distribution results for the internal energies of the ions in the ICR cell, from the equilibration to a steady-state.^{120,121} These circumstances allow for kinetic parameters to be determined by the dissociation process, giving a measure of the stabilities of the gas-phase ions. Dissociation rate constants can be calculated from the comparison of fragmentation yields at different activation times. If the above experiment is performed at several temperatures, the activation energy and the pre-exponential Arrhenius factor are easily calculated. The Arrhenius equation states that

$$k = Ae^{-E_a/RT}$$

where k represents the rate constant, A is the pre-exponential Arrhenius factor, E_a is the activation energy, R is the gas constant and T is the absolute temperature of the ICR cell. When we consider large molecules, E_a is assumed to be equal to the threshold energy for dissociation (E_0).¹²² Unimolecular dissociation rate constants (k_{diss}) are easily derived for BIRD data. Once k_{diss} has been found at several temperatures, a plot of $\ln k_{\text{diss}}$ vs $1/T$ provides the activation constant (E_a) and the Arrhenius constant (A) for the dissociation of the precursor. Figure 13 illustrates how these parameters are found from BIRD data.

The information gained from BIRD experiments can help investigate the nature of the fragmentation mechanisms involved. The pre-exponential factor for a unimolecular reaction is

$$A = \frac{k_b T}{h} e^{\left(1 + \frac{\Delta S_0^*}{R}\right)}$$

where k_b is the Boltzmann constant, h is Planck's constant and ΔS_0^* represent the entropy difference between the transition state and the precursor structure. Direct bond cleavages result in A values ranging from 10^{15} to 10^{18} s^{-1} .¹²³ Conversely, rearrangements have much lower Arrhenius constants (10^{10} – 10^{13} s^{-1}).¹²³ Rearrangements have tight transition-state geometries, hence their entropy factors are low. The opposite is true for entropically favored simple bond cleavages.

Unfortunately, the working temperature for BIRD must remain below 200°C , since severe problems with the FTICR can occur above this temperature, including an increase in cryogen boil-off and a rise in pressure inside the ICR cell.¹²⁴ Nonetheless, important information on the dissociative properties of ions trapped in the cell can still be gained in this limited temperature range. Another disadvantage of BIRD is that very long times are needed (up to hours) to equilibrate the ICR cell thermally to the desired temperature. Also, experiments are not easily performed when initially 'cold' ions are needed, such as H/D exchange studies. As a result, an alternative method has been deduced using CO_2 laser irradiation (IRMPD) for the determination of gas-phase activation energies of biomolecules.¹²⁴ Advantages of this method include an increase in the 'effective' temperature range and the application to a wider range of problems, since heat is transferred extremely fast and therefore dissociation is much more rapid. BIRD currently consists of the slowest ion activation technique in MS/MS with heating times ranging from seconds to several minutes.³⁵ It is consequently usually incompatible with coupled separation techniques, such as liquid chromatography or capillary electrophoresis. The most common application for BIRD is the calculation of kinetic parameters of dissociation for large molecules, such as oligonucleotides¹²⁵ and proteins.^{119,126} Multiprotein complex stabilities have also been examined by measuring the temperature dependence of the dissociation rate constants.¹²⁷ BIRD represents the only activation technique with a direct thermal analogy for facile calculations of kinetic parameters.

CONCLUSION

The use of ion activation in MS/MS has evolved, over the past 40 years, into a collection of several powerful techniques. Historically, the dissociative properties of gaseous ions were studied by fragmentations occurring either in the ion source, by electron ionization, or by metastable decompositions taking place during an ion's flight from the source to the detector. Once it was realized that a much wider range of molecules could be analyzed by using soft ionization techniques, the need for separate activation methods became apparent. CID can currently be performed, at either low or high collision energies, in all common MS configurations and is the most frequently used approach for ion activation.

More recently, several innovative techniques have been developed, each with its own specific advantages and applications. SID is very similar to CID, but allows increased control for energy deposition and can, at times, lead to increased fragmentation, especially for large ions with high dissociation thresholds. ECD is a unique technique for the observation of non-ergodic dissociation behavior of multiply charged cations and exhibits distinct fragmentation mechanisms. IRMPD employs IR radiation, usually by the use of low-power continuous-wave CO_2 lasers, in order to cause fragmentation of ions in trapping instruments. Finally, BIRD can thermally activate ions in FT-ICR instruments. It allows the determination of activation energies and Arrhenius constants for dissociation reactions, and can ultimately assist in the elucidation of specific fragmentation mechanisms. These activation techniques can be used separately or in combination to yield very interesting and comprehensive results. Mass spectrometry has, in our opinion, become the key enabling technology for investigating biological and biochemical mechanisms today. While it is in a constant flux with innovations, the availability of a range of well-established ion activation technologies is extremely useful in both fundamental studies and specific applications.

Acknowledgement

The authors thank Dr Graham Cooks for helpful suggestions during the course of the reviewing process of this manuscript.

REFERENCES

1. Barber M, Bordoli RS, Sedgwick RD. In *Soft Ionization Biological Mass Spectrometry*, Morris HR (ed). Heyden: London, 1981; 137.
2. Yamashita M, Fenn JB. Electrospray ion source. Another variation on the free-jet theme. *J. Phys. Chem.* 1984; **88**: 4451.
3. Yamashita M, Fenn JB. Negative ion production with the electrospray source. *J. Phys. Chem.* 1984; **88**: 4671.
4. Karas M, Bachmann D, Bahr U, Hillenkamp F. Matrix-assisted ultraviolet laser desorption of non-volatile compounds. *Int. J. Mass Spectrom. Ion Processes* 1987; **78**: 53.
5. Lorquet JC. In *The Structure, Energetics and Dynamics of Organic Ions*, Baer T, Ng CY, Powis I (eds). Wiley: Chichester, 1996; 167.
6. Rosenstock HM, Wallenstein MB, Wahrhartig A, Eyring H. Absolute rate theory for isolated systems and the mass spectra of polyatomic molecules. *Proc. Natl. Acad. Sci. USA.* 1952; **38**: 667.
7. Marcus RA. Unimolecular dissociations and free radical recombination reactions. *J. Chem. Phys.* 1952; **20**: 359.
8. Longevialle P. In *Principes de la Spectrometrie de Masse des Substances Organiques*. Masson: Paris, 1981; 21.
9. Gilbert RG, Smith SC. In *Theory of Unimolecular and Recombination Reactions*. Blackwell: Oxford, 1990; 52.
10. McLafferty FW, Tureček F. In *Interpretation of Mass Spectra* (4th edn). University Science Books: Mill Valley, CA, 1993; Ch. 7 (McLafferty rearrangement, radical ion fragmentations), 116 (metastable ions), 138 (relative fragmentation energies).
11. Williams DH, Cooks RG. The role of 'frequency factors' in determining the difference between low- and high-voltage mass spectra. *Chem. Commun.* 1968; 663.
12. Aston FW. The distribution of intensity along the positive ray parabolas of atoms and molecules of hydrogen and its possible explanation. *Proc. Cambridge Philos. Soc.* 1919; **19**: 317.
13. Hipple JA, Condon EU. Detection of metastable ions with the mass spectrometer. *Phys. Rev.* 1945; **68**: 54.
14. Spitteller G, Spitteller-Friedmann M. Vergleichende massenspektrometrische Untersuchung einiger Purinderivate. *Monatsh. Chem.* 1962; **93**: 632.

15. de Hoffmann E, Stroobant V. In *Mass Spectrometry. Principles and Applications* (2nd edn). Wiley: Chichester 2002; 108, 246.
16. Spengler B, Kirsch D, Kaufmann R. Fundamentals of post source decay in MALDI-MS. 1. Residual gas effects. *J. Phys. Chem.* 1992; **96**: 9678.
17. Kaufmann R, Kirsh D, Spengler B. Sequencing of peptides in a time-of-flight mass spectrometer: evaluation of postsorce decay following matrix-assisted laser desorption ionization (MALDI). *Int. J. Mass Spectrom. Ion Processes* 1994; **131**: 355.
18. Karas M, Hillenkamp F. Laser desorption ionization of proteins with molecular masses exceeding 10000 daltons. *Anal. Chem.* 1988; **60**: 2299.
19. Kaufmann R, Spengler B, Lützenkirchen F. Mass spectrometric sequencing of linear peptides by product-ion analysis in a reflectron time-of-flight mass spectrometer using matrix-assisted laser desorption ionization. *Rapid Commun. Mass Spectrom.* 1993; **7**: 902.
20. Beynon JH, Cooks RG, Amy JM, Baitinger WE, Ridley TY. Design and performance of a mass-analysed ion kinetic energy (MIKE) spectrometer. *Anal. Chem.* 1973; **45**: 1023A.
21. Walton TJ, Bayliss MA, Pereira ML, Games DE, Genieser H-G, Brenton AG, Harris FM, Newton RP. Fast-atom bombardment tandem mass spectrometry of cyclic nucleoside analogues used as site-selective activators of cyclic nucleotide-dependent protein kinases. *Rapid Commun. Mass Spectrom.* 1998; **12**: 449.
22. Frański R, Gierczyk B, Fiedorow P, Chadyniak D, Urbaniak W. Investigation of 4-(nitrophenylamino)pent-3-en-2-ones and 4-(nitrobenzylamino)pent-3-en-2-ones by electron ionization mass spectrometry. Observation of characteristic *ortho* effects. *Eur. J. Mass Spectrom.* 2003; **9**: 465.
23. Cooks RG, Beynon JH, Caprioli RM, Lester GR. *Metastable Ions*. Gross ML (ed.). Elsevier: Amsterdam 1973; 57.
24. Bruins AP, Jennings KR. The observation of metastable transitions in a double-focusing mass spectrometer using a linked scan of the electric sector and magnetic sector fields. *Int. J. Mass Spectrom.* 1978; **26**: 395.
25. Jenning KR. *High Performance Mass Spectrometry: Chemical Applications: a Symposium*. American Chemical Society: Washington, DC, 1978; 3.
26. Boyd RK, Porter CJ, Beynon JH. A new linked scan for reversed geometry mass spectrometers. *Org. Mass Spectrom.* 1981; **16**: 493.
27. Haddon WF. The constant neutral linked magnetic field-electric sector scan. *Org. Mass Spectrom.* 1980; **15**: 539.
28. McLuckey SA. Principles of collisional activation in analytical mass spectrometry. *J. Am. Soc. Mass Spectrom.* 1992; **3**: 599.
29. Shukla AK, Futrell JH. Tandem mass spectrometry: dissociation of ions by collisional activation. *J. Mass Spectrom.* 2000; **35**: 1069.
30. Jennings KR. The changing impact of the collision-induced decomposition of ions on mass spectrometry. *Int. J. Mass Spectrom.* 2000; **200**: 479.
31. Levsen K. In *Fundamental Aspects of Organic Mass Spectrometry*. Verlag Chemie: Weinheim, 1978; 138 (collision process), 92 (energy dependence of CID products).
32. Cooks RG. In *Collision Spectroscopy*. Plenum Press: New York, 1979; 8 (Newton diagrams), 372 (QET fragmentation).
33. Busch KL, Glish GL, McLuckey SA. In *Mass Spectrometry/Mass Spectrometry: Techniques and Applications of Tandem Mass Spectrometry*. VCH: New York, 1988; 64 (E_{com}), 84 (pressure effects).
34. Durup J. In *Recent Developments in Mass Spectrometry*, Ogata K, Hayakawa T (eds). University Park Press: Baltimore, MD, 1970; 921.
35. McLuckey SA, Goeringer DE. Slow heating methods in tandem mass spectrometry. *J. Mass Spectrom.* 1997; **32**: 461.
36. Gauthier JW, Trautman TR, Jacobson DB. Sustained off-resonance irradiation for collision-activated dissociation involving Fourier transform mass spectrometry. Collision-activated dissociation technique that emulates infrared multiphoton dissociation. *Anal. Chim. Acta* 1991; **246**: 211.
37. Schwartz RN, Slawsky ZI, Herzfeld KF. Calculation of vibrational relaxation times in gases. *J. Chem. Phys.* 1952; **20**: 1591.
38. Volmer DA, Mansoori B, Locke SJ. Study of 4-quinolone antibiotics in biological samples by short-column liquid chromatography coupled with electrospray ionization tandem mass spectrometry. *Anal. Chem.* 1997; **69**: 4143.
39. Chace DH, Hillman SL, Millington DS, Kahler SG, Adam BW, Levy HL. Rapid diagnosis of homocystinuria and other hypermethioninemias from newborns' blood spots by tandem mass spectrometry. *Clin. Chem.* 1996; **42**: 349.
40. Hager JM, Le Blanc JCY. Product ion scanning using a Q-q-Q_{linear} ion trap (Q TRAPTM) mass spectrometer. *Rapid Commun. Mass Spectrom.* 2003; **17**: 1056.
41. Chernushevich IV, Loboda AV, Thomson BA. An introduction to quadrupole-time-of-flight mass spectrometry. *J. Mass Spectrom.* 2001; **36**: 849.
42. Akashi S, Takio K. Structure of melittin bound to phospholipid micelles studied using hydrogen-deuterium exchange and electrospray ionization Fourier transform ion cyclotron resonance mass spectrometry. *J. Am. Soc. Mass Spectrom.* 2001; **12**: 1247.
43. Olsen JV, Ong S-E, Mann M. Trypsin cleaves exclusively C-terminal to arginine and lysine residues. *Mol. Cell. Proteomics* 2004; **3**: 608.
44. Spengler B. Post-source decay analysis in matrix-assisted laser desorption/ionization mass spectrometry of biomolecules. *J. Mass Spectrom.* 1997; **32**: 1019.
45. Cotter RJ. In *Time-of-Flight Mass Spectrometry: Instrumentation and Applications in Biological Research*. American Chemical Society: Washington, DC, 1997; 204.
46. Yamaoka H, Pham D, Durup J. Energetics of the collision-induced dissociations $C_2H_2^+ \rightarrow C_2H^+ + H$ and $C_2H_2^+ \rightarrow H^+ + C_2H$. *J. Chem. Phys.* 1969; **51**: 3465.
47. Franchetti V, Freiser BS, Cooks RG. Excitation in ion-molecule collisions. A study of protonated aromatic molecules by ion kinetic energy spectrometry. *Org. Mass Spectrom.* 1978; **13**: 106.
48. Beynon JH, Boyd RK, Brenton AG. In *Advances in Mass Spectrometry (1985)*, Todd JFJ (ed). Wiley: New York, 1986; 437.
49. Wysocki V, Kenttämää HI, Cooks RG. Internal energy distributions of isolated ions after activation by various methods. *Int. J. Mass Spectrom. Ion Processes* 1987; **75**: 181.
50. Biemann K. Contributions of mass spectrometry to peptide and protein structure. *Biomed. Environ. Mass Spectrom.* 1988; **16**: 99.
51. Papayannopoulos IA. The interpretation of collision-induced dissociation tandem mass spectra of peptides. *Mass Spectrom. Rev.* 1995; **14**: 49.
52. Schlosser A, Lehmann WD. Five-membered ring formation in unimolecular reactions of peptides: a key structural element controlling low-energy collision-induced dissociation of peptides. *J. Mass Spectrom.* 2000; **35**: 1382.
53. Fabris D, Kelly M, Murphy C, Wu Z, Fenselau C. High-energy collision-induced dissociation of multiply charged polypeptides produced by electrospray. *J. Am. Soc. Mass Spectrom.* 1993; **4**: 652.
54. Cooks RG, Ast T, Beynon JH. Anomalous metastable peaks. *Int. J. Mass Spectrom. Ion Phys.* 1975; **16**: 348.
55. Cooks RG, Ast T, Mabud MdA. Collisions of polyatomic ions with surfaces. *Int. J. Mass Spectrom. Ion Processes* 1990; **100**: 209.
56. Williams ER, Henry KD, McLafferty FW, Shabanowitz J, Hunt DF. Surface-induced dissociation of peptide ions in Fourier-transform mass spectrometry. *J. Am. Soc. Mass Spectrom.* 1990; **1**: 413.
57. Chorush RA, Little DP, Beu SC, Wood TD, McLafferty FW. Surface-induced dissociation of multiply-protonated proteins. *Anal. Chem.* 1995; **67**: 1042.
58. Schaaff TG, Qu Y, Farrell N, Wysocki VH. Investigation of the *trans* effect in the fragmentation of dinuclear platinum complexes by electrospray ionization surface-induced

- dissociation tandem mass spectrometry. *J. Mass Spectrom.* 1998; **33**: 436.
59. Nair H, Somogyi Á, Wysocki VH. Effect of alkyl substitution at the amide nitrogen on amide bond cleavage: electrospray ionization/surface-induced dissociation fragmentation of substance P and two alkylated analogs. *J. Mass Spectrom.* 1996; **31**: 1141.
 60. Dongré AR, Somogyi Á, Wysocki VH. Surface-induced dissociation: an effective tool to probe structure, energetics and fragmentation mechanisms of protonated peptides. *J. Mass Spectrom.* 1996; **31**: 339.
 61. Laskin J, Denisov EV, Shukla AK, Barlow SE, Futrell JH. Surface-induced dissociation in a Fourier transform ion cyclotron resonance mass spectrometer: instrument design and evaluation. *Anal. Chem.* 2002; **74**: 3255.
 62. Laskin J, Bailey TH, Futrell JH. Shattering of peptide ions on self-assembled monolayer surfaces. *J. Am. Chem. Soc.* 2003; **125**: 1625.
 63. Laskin J, Beck KM, Hache JJ, Futrell JH. Surface-induced dissociation of ions produced by matrix-assisted laser desorption/ionization in a Fourier transform ion cyclotron resonance mass spectrometer. *Anal. Chem.* 2004; **76**: 351.
 64. Laskin J, Futrell JH. Collisional activation of peptide ions in FT-ICR mass spectrometry. *Mass Spectrom. Rev.* 2003; **22**: 158.
 65. Grill V, Shen J, Evans C, Cooks RG. Collisions of ions with surfaces at chemically relevant energies: instrumentation and phenomena. *Rev. Sci. Instrum.* 2001; **72**: 3149.
 66. Franchetti V, Solka BH, Baitinger WE, Amy JW, Cooks RG. Soft landing of ions as a means of surface modification. *Int. J. Mass Spectrom. Ion Phys.* 1977; **23**: 29.
 67. Laskin J, Futrell JH. Surface-induced dissociation of peptide ions: kinetics and dynamics. *J. Am. Soc. Mass Spectrom.* 2003; **14**: 1340.
 68. Schulz DG, Lim H, Garbis S, Hanley L. Energy partitioning in the surface-induced dissociation of linear and cyclic protonated peptides at an organic surface. *J. Mass Spectrom.* 1999; **34**: 217.
 69. Wysocki VH, Ding J-M, Jones JL, Callahan JH, King FL. Surface-induced dissociation in tandem quadrupole mass spectrometers: a comparison of three designs. *J. Am. Soc. Mass Spectrom.* 1992; **3**: 27.
 70. Meroueh O, Hase WL. Dynamics of energy transfer in peptide-surface collisions. *J. Am. Soc. Chem.* 2002; **124**: 1524.
 71. Murata Y. In *Unimolecular and Bimolecular Ion–Molecule Reaction Dynamics*, Ng CY, Baer T, Powis I (eds). Wiley: Chichester, 1994; 427.
 72. Ast T, Mabud MdA, Cooks RG. Reactive collisions of polyatomic ions at solid surfaces. *Int. J. Mass Spectrom. Ion Processes* 1988; **82**: 131.
 73. Hayward MJ, Mabud MdA, Cooks RG. Ion/surface collisions for distinction of isomeric $[C_6H_6]^{+}$ and $[C_6H_6]^{2+}$ ions. *J. Am. Soc. Chem.* 1988; **110**: 1343.
 74. Somogyi Á, Kane TE, Ding J-M, Wysocki VH. Reactive collisions of $C_6H_6^{+}$ and $C_6D_6^{+}$ at self-assembled monolayer films prepared on gold from n-alkanethiols and a fluorinated alkanethiol: the influence of chain length on the reactivity of the films and the neutralization of the projectile. *J. Am. Chem. Soc.* 1993; **115**: 5275.
 75. Kane TE, Somogyi Á, Wysocki VH. Reactive ion–surface collisions: application of ionized acetone- d_6 , DMSO- d_6 and pyridine- d_5 as probes for the characterization of self-assembled monolayer films on gold. *Org. Mass Spectrom.* 1993; **28**: 1665.
 76. Bier ME, Amy JW, Cooks RG, Syka JEP, Ceja P, Stafford G. A tandem quadrupole mass spectrometer for the study of surface-induced dissociation. *Int. J. Mass Spectrom. Ion Processes* 1987; **77**: 31.
 77. Schey K, Cooks RG, Grix R, Wollnik H. A tandem time-of-flight mass spectrometer for surface-induced dissociation. *Int. J. Mass Spectrom. Ion Processes* 1987; **77**: 49.
 78. Williams ER, Fang L, Zare RN. Surface induced dissociation for tandem time-of-flight mass spectrometry. *Int. J. Mass Spectrom. Ion Processes* 1993; **123**: 233.
 79. Schey KL, Cooks RG, Kraft A, Grix R, Wollnik H. Ion/surface collision phenomena in an improved tandem time-of-flight instrument. *Int. J. Mass Spectrom. Ion Processes* 1989; **94**: 1.
 80. Beck RD, St. John P, Homer ML, Whetten RL. Impact-induced cleaving and melting of alkali-halide nanocrystals. *Science* 1991; **253**: 879.
 81. St. John PM, Beck RD, Whetten RL. Reactions in cluster-surface collisions. *Phys. Rev. Lett.* 1992; **69**: 1467.
 82. St. John PM, Whetten RL. Hyperthermal collisions of silicon clusters with solid surfaces. *Chem. Phys. Lett.* 1992; **196**: 330.
 83. Ijames CF, Wilkins CL. Surface-induced dissociation by Fourier transform mass spectrometry. *Anal. Chem.* 1990; **62**: 1295.
 84. Castoro JA, Nuwaysir LM, Ijames CF, Wilkins CL. Comparative study of photodissociation and surface-induced dissociation by laser desorption Fourier transform mass spectrometry. *Anal. Chem.* 1992; **64**: 2238.
 85. Lammert SA, Cooks RG. Surface-induced dissociation of molecular ions in a quadrupole ion trap mass spectrometer. *J. Am. Soc. Mass Spectrom.* 1991; **2**: 487.
 86. McLafferty FW, Amster IJ, Furlong JJP, Loo JA, Wang BH, Williams ER. In *Fourier Transform Mass Spectrometry: Evolution Innovation and Applications*. ACS Symposium Series, No. 359, Buchanan MV (ed). American Chemical Society: Washington, DC, 1987; 116.
 87. Zubarev RA, Kelleher NL, McLafferty FW. Electron capture dissociation of multiply charged protein cations. A nonergodic process. *J. Am. Soc. Chem.* 1998; **120**: 3265.
 88. Zubarev RA, Haselmann KF, Budnik B, Kjeldsen F, Jensen F. Towards an understanding of the mechanism of electron-capture dissociation: a historical perspective and modern ideas. *Eur. J. Mass Spectrom.* 2002; **8**: 337.
 89. McLafferty FW, Horn DM, Breuker K, Ge Y, Lewis MA, Cerda B, Zubarev RA, Carpenter BK. Electron capture dissociation of gaseous multiply charged ions by Fourier-transform ion cyclotron resonance. *J. Am. Soc. Mass Spectrom.* 2001; **12**: 245.
 90. Haselmann KF, Budnik BA, Olsen JV, Nielsen ML, Reis CA, Clausen H, Johnson AH, Zubarev RA. Advantages of external accumulation for electron capture dissociation in Fourier transform mass spectrometry. *Anal. Chem.* 2001; **73**: 2998.
 91. Zubarev RA. Reactions of polypeptide ions with electrons in the gas phase. *Mass Spectrom. Rev.* 2003; **22**: 57.
 92. Bardsley JN, Bionidi MA. In *Advances in Atomic and Molecular Physics*, vol. 6, Bates DR (ed). Academic Press: New York, 1970; 5.
 93. Zubarev RA, Horn DM, Fridriksson EK, Kelleher NL, Kruger NA, Lewis MA, Carpenter BK, McLafferty FW. Electron capture dissociation for structural characterization of multiply charged protein cations. *Anal. Chem.* 2000; **72**: 563.
 94. Kjeldsen F, Haselmann KF, Budnik BA, Jensen F, Zubarev RA. Dissociation capture of hot (3–13 eV) electrons by polypeptide polycations: an efficient process accompanied by secondary fragmentation. *Chem. Phys. Lett.* 2002; **356**: 201.
 95. Tureček F, McLafferty FW. Non-ergodic behavior in acetone-enol ion dissociations. *J. Am. Chem. Soc.* 1984; **106**: 2525.
 96. Horn DM, Ge Y, McLafferty FW. Activated ion electron capture dissociation for mass spectral sequencing of larger (42 kDa) proteins. *Anal. Chem.* 2000; **72**: 4778.
 97. Cerda BA, Horn DM, Breuker K, Carpenter BK, McLafferty FW. Electron capture dissociation of multiply charged oxygenated cations. A nonergodic process. *Eur. J. Mass Spectrom.* 1999; **5**: 335.
 98. Cerda BA, Breuker K, Horn DM, McLafferty FW. Charge/radical site initiation versus coulombic repulsion for cleavage of multiply charged ions. Charge solvation in poly(alkene glycol) ions. *J. Am. Soc. Mass Spectrom.* 2001; **12**: 565.
 99. Olsen JV, Haselmann KF, Nielsen ML, Budnik BA, Nielsen PE, Zubarev RA. Comparison of electron capture dissociation and collisionally activated dissociation of polycations of peptide nucleic acids. *Rapid Commun. Mass Spectrom.* 2001; **15**: 969.

100. Håkansson K, Hudgins RR, Marshall AG, O'Hair RAJ. Electron capture dissociation and infrared multiphoton dissociation of oligodeoxynucleotide dications. *J. Am. Soc. Mass Spectrom.* 2003; **14**: 23.
101. Håkansson K, Cooper HJ, Emmett MR, Costello CE, Marshall AG, Nilsson CL. Electron capture dissociation and infrared multiphoton dissociation MS/MS of an *N*-glycosylated tryptic peptide to yield complementary sequence information. *Anal. Chem.* 2001; **73**: 4530.
102. Thorne LR, Beauchamp JL. In *Gas Phase Ion Chemistry*. Vol. 3: *Ions and Light*, MT Bowers (ed). Academic Press: London, 1984; 41.
103. van der Hart WJ. Studies of ion structures by photodissociation. *Int. J. Mass Spectrom. Ion Processes* 1992; **118/119**: 617.
104. Uechi GT, Dunbar RC. The kinetics of infrared laser photodissociation of *n*-butylbenzene ions at low pressure. *J. Chem. Phys.* 1992; **96**: 8897.
105. Colorado A, Shen JX, Vartanian VH, Brodbelt J. Use of infrared multiphoton photodissociation with SWIFT for electrospray ionization and laser desorption applications in a quadrupole ion trap mass spectrometer. *Anal. Chem.* 1996; **68**: 4033.
106. Marshall AG, Wang TCL, Ricca TL. Tailored excitation for Fourier transform ion cyclotron resonance mass spectrometry. *J. Am. Chem. Soc.* 1985; **107**: 7893.
107. Hofstadler SA, Sannes-Lowery KA, Griffey RH. Infrared multiphoton dissociation in an external ion reservoir. *Anal. Chem.* 1999; **71**: 2067.
108. Hofstadler SA, Drader JJ, Gaus H, Hannis JC, Sannes-Lowery KA. Alternative approaches to infrared multiphoton dissociation in an ion external reservoir. *J. Am. Soc. Mass Spectrom.* 2003; **14**: 1413.
109. Little DP, Speir JP, Senko MW, O'Connor PB, McLafferty FW. Infrared multiphoton dissociation of large multiply charged ions for biomolecule sequencing. *Anal. Chem.* 1994; **66**: 2809.
110. Li W, Hendrickson CL, Emmett MR, Marshall AG. Identification of intact proteins in mixtures by alternated capillary liquid chromatography electrospray ionization and LC ESI infrared multiphoton dissociation Fourier transform ion cyclotron resonance mass spectrometry. *Anal. Chem.* 1999; **71**: 4397.
111. Xie Y, Lebrilla CB. Infrared multiphoton dissociation of alkali metal-coordinated oligosaccharides. *Anal. Chem.* 2003; **75**: 1590.
112. Little DP, Aaserud DJ, Valaskovic GA, McLafferty FW. Sequence information from 42–108-mer DNAs (complete for a 50-mer) by tandem mass spectrometry. *J. Am. Chem. Soc.* 1996; **118**: 9352.
113. Sannes-Lowery KA, Hofstadler SA. Sequence confirmation of modified oligonucleotides using IRMPD in the external ion reservoir of an electrospray ionization Fourier transform ion cyclotron mass spectrometer. *J. Am. Soc. Mass Spectrom.* 2003; **14**: 825.
114. Goolsby BJ, Brodbelt JS. Analysis of protonated and alkali metal cationized aminoglycoside antibiotics by collision-activated dissociation and infrared multiphoton dissociation in the quadrupole ion trap. *J. Mass Spectrom.* 2000; **35**: 1011.
115. Crowe MC, Brodbelt JS, Goolsby BJ, Hergenrother P. Characterization of erythromycin analogs by collisional activated dissociation and infrared multiphoton dissociation in a quadrupole ion trap. *J. Am. Soc. Mass Spectrom.* 2002; **13**: 630.
116. Håkansson K, Chalmers MJ, Quinn JP, McFarland MA, Hendrickson CL, Marshall AG. Combined electron capture and infrared multiphoton dissociation for multistage MS/MS in a Fourier transform ion cyclotron resonance mass spectrometer. *Anal. Chem.* 2003; **75**: 3256.
117. Tsybin YO, Witt M, Bayhut G, Kjeldsen F, Håkansson P. Combined infrared multiphoton dissociation and electron capture dissociation with a hollow electron beam in Fourier transform ion cyclotron resonance mass spectrometry. *Rapid Commun. Mass Spectrom.* 2003; **17**: 1759.
118. Hashimoto Y, Hasegawa H, Yoshinari K, Waki I. Collision-activated infrared multiphoton dissociation in a quadrupole ion trap mass spectrometer. *Anal. Chem.* 2003; **75**: 420.
119. Price WD, Schnier PD, Williams ER. Tandem mass spectrometry of large biomolecule ions by blackbody infrared radiative dissociation. *Anal. Chem.* 1996; **68**: 859.
120. Price WD, Schnier PD, Jockusch RA, Strittmatter EF, Williams ER. Unimolecular reaction kinetics in the high-pressure limit without collisions. *J. Am. Chem. Soc.* 1996; **118**: 10640.
121. Price WD, Williams ER. Activation of peptide ions by blackbody radiation: factors that lead to dissociation kinetics in the rapid energy exchange limit. *J. Phys. Chem. A* 1997; **101**: 8844.
122. Dunbar RC, McMahon TB. Activation of unimolecular reactions by ambient blackbody radiation. *Science* 1998; **279**: 194.
123. Benson SW. In *Thermochemical Kinetics. Methods for the Estimation of Thermochemical Data and Rate Parameters*. Wiley: New York, 1968; 70, 80.
124. Freitas MA, Hendrickson CL, Marshall AG. Gas phase activation energy for unimolecular dissociation of biomolecular ions determined by focused radiation for gaseous multiphoton energy transfer (FRAGMENT) *Rapid Commun. Mass Spectrom.* 1999; **13**: 1639.
125. Klassen JS, Schnier PD, Williams ER. Blackbody infrared radiative dissociation of oligonucleotide anions. *J. Am. Soc. Mass Spectrom.* 1998; **9**: 1117.
126. Jockusch RA, Schnier PD, Price WD, Strittmatter EF, Demirev PA, Williams ER. Effects of charge state on fragmentation pathways, dynamics, and activation energies of ubiquitin ions measured by blackbody infrared radiative dissociation. *Anal. Chem.* 1997; **69**: 1119.
127. Felitsyn N, Kitova EN, Klassen JS. Thermal decomposition of a gaseous multiprotein complex studied by blackbody infrared radiative dissociation. Investigating the origin of the asymmetric dissociation behavior. *Anal. Chem.* 2001; **73**: 4647.

APPENDIX 1.

List of Symbols and Physical Constants

<i>A</i>	Arrhenius constant
<i>B</i>	Magnetic field strength
ΔS^\ddagger	Entropy factor for the transition state
eV	Electronvolt (1 eV = 96.48 kJ mol ⁻¹)
<i>E</i>	Electric field strength
<i>E_a</i>	Arrhenius activation energy
<i>E_k</i>	Kinetic energy
<i>E_{com}</i>	Center of mass energy
<i>E_{lab}</i>	Laboratory collision energy
<i>E₀</i>	Threshold energy
<i>h</i>	Planck's constant
<i>k</i>	Rate constant
<i>k_b</i>	Boltzmann's constant
<i>m</i>	Mass of an ion
<i>m_p</i>	Precursor ion mass
<i>m_f</i>	Fragment ion mass
<i>m*</i>	Apparent mass of metastable ions
<i>n</i>	Number of vibrational degrees of freedom
<i>N</i>	Mass of the neutral target
<i>P[≠]</i>	Total number of states of activated complexes
ρ_E	Density of states of an ion at energy <i>E</i>
<i>q</i>	Endothermicity
<i>q_z</i>	Contribution in <i>z</i> -direction of dimensionless parameter in Mathieu equation
<i>r_b</i>	Radius of an ion's trajectory in the magnetic sector
<i>r_e</i>	Radius of an ion's trajectory in the electrostatic sector
<i>R</i>	Gas constant
<i>T</i>	Temperature (K)

ν	Frequency factor
ν	Frequency of photon
v	Velocity of an ion
V_{acc}	Accelerating voltage
z	Charge state of the ion
Z	Partition function for adiabatic degrees of freedom

APPENDIX 2.

Abbreviations

B	Magnetic sector	IR	Infrared
BE	Double-focusing sector in reverse geometry	IRMPD	Infrared multiphoton dissociation
B/E	Product ion scan on double-focusing sector instrument	IT	Ion trap
B ² /E	Precursor ion scan on double-focusing sector instrument	MALDI	Matrix-assisted laser desorption/ionization
BIRD	Blackbody infrared irradiative dissociation	MIKES	Mass-analyzed ion kinetic energy spectroscopy
BqQ	Hybrid sector-quadrupole	MS/MS	Tandem mass spectrometry
CID	Collision-induced dissociation	MS ⁿ	Tandem mass spectrometry in an ion trap (<i>n</i> th generation MS/MS)
com	Center of mass reference frame	QET	Quasi-equilibrium theory
E	Electrostatic sector	Q	Quadrupole
EB	Double-focusing sector in normal geometry	q	Collision quadrupole in hybrid instruments (operated in r.f.-only mode)
ECD	Electron capture dissociation	QqQ	Triple-quadrupole
EI	Electron ionization	QqLIT	Quadrupole linear ion trap
FTICR	Fourier transform ion cyclotron resonance	QqTOF	Quadrupole time-of-flight
		PSD	Post-source decay
		RETOF	Reflectron-TOF
		r.f.	Radiofrequency
		RRKM	Rice, Ramsberger, Kassel, Marcus
		SAM	Self-assembled monolayer
		SID	Surface-induced dissociation
		SORI	Sustained off resonance irradiation
		TOF/TOF	Tandem time-of-flight instrument
		TOF	Time-of-flight
		UV	Ultraviolet